introducing lipophilic groups in the C-7 position, in particular chlorine, significantly improves PAFR affinity compared to GB (**1**). This gives rise to new possibilities for improving affinity of ginkgolides to PAFR, as well as providing material for future SAR studies of ginkgolides and PAFR.

Experimental Section

Chemistry. General Procedures. GB (**1**) and GC (**2**) was obtained by extraction of leaves from *G. biloba*, purification by column chromatography and recrystallization as previously described.[31,32] The purity was >98% as estimated by ^{1}H NMR. Unless otherwise noted, materials were obtained from a commercial supplier and were used without further purification. Solvents were dried by eluting through alumina columns. Flash column chromatography was performed using ICN silica gel (32−63 mesh). Thin-layer chromatography was carried out using precoated silica gel 60 F_{254} plates with thickness of 0.25 mm. Plates were heated and spots were detected by monitoring at 254 nm. ^{1}H and ^{13}C NMR spectra were obtained on Bruker DMX 300 MHz or Bruker DMX 400 MHz spectrometers and are reported in parts per million (ppm) relative to internal solvent signal, with coupling constants (J) in hertz (Hz). HSQC, COSY, and ROESY spectra were obtained on a Bruker DMX 400 MHz or Bruker DMX 500 MHz spectrometer. Analytical and preparative high performance liquid chromatography (HPLC) were performed on a HP 1100 LC instrument with detection by UV at 219 and 254 nm. Preparative HPLC was performed using a 10 μm C18 reversed-phase VYDAC column (250 × 22 mm) with a flow of 4 mL/min and eluting with either eluent A or B. A: water/CH_3CN/TFA (60:40:0.1), raising to (40:60:1) after 20 min. B: water/CH_3CN/TFA (65:35:0.1), raising to (40:60:1) after 20 min. Analytical HPLC were performed using a 5 μm C18 reversed-phase Phenomenex Luna column (150 × 4.60 mm), with a flow of 1 mL/min eluting with water/CH_3CN/TFA 70:30:0.1. Compounds **9** and **14** were eluted with water/CH_3CN/TFA 80:20:0.10 and compounds **11**−**13** with water/CH_3CN 90:10. Accurate mass determinations were performed on a JEOL JMS−HX110/100A HF mass spectrometer using a 3-nitrobenzyl alcohol (NBA) matrix and Xe ionizing gas and are within ±10 ppm of theoretical values. All were crystalline compounds that decompose above 200 °C

7-Trifluoromethanesulfonyloxy Ginkgolide B (3). In a mixture of dry CH_2Cl_2 (1.0 mL) and dry pyridine (1.5 mL) was dissolved GC (**2**) (184 mg, 0.42 mmol). The solution was cooled to −20 °C under argon, and trifluoromethane sulfonic anhydride (78 μL) was added dropwise. The reaction was stirred at −20 °C for 2 h and allowed to warm to room temperature over 1 h. The solvent was removed in vacuo, the residue was dissolved in EtOAc (30 mL) and washed with 1 N HCl (3 × 20 mL) and brine (10 mL) and dried ($MgSO_4$), and the solvent was removed in vacuo. The crude product was purified by flash chromatography eluting with $CHCl_3$/CH_3OH/EtOAc (30:1:1 and 20:1:1) to obtain **3** as white crystals (232 mg, 97%). ^{1}H NMR (400 MHz, DMSO-d_6): δ 1.11 (s, *tert*-butyl), 1.13 (d, J = 9.6, CH_3), 2.22 (d, J = 16.5, 8-H), 2.82 (q, J = 9.6, 14-H), 4.15 (dd, J = 8.0, 5.9, 1-H), 4.73 (d, J = 8.0, 2-H), 5.08 (d, J = 7.4, 10-H), 5.24 (dd, J = 16.5, 5.6, 7-H) 5.41 (d, J = 5.6, 6-H), 5.54 (d, J = 5.9, 1-OH), 6.20 (s, 12-H), 6.62 (s, 3-OH), 7.63 (d, J = 7.4, 10-OH). ^{13}C NMR (100 MHz, DMSO-d_6): δ 9.1, 29.2 (3C), 32.6, 42.1, 49.0, 64.2, 68.1, 69.4, 74.4, 75.2, 84.0, 86.3, 93.2, 99.9, 109.4, 118.6 (q, $^1J_{CF}$ = 316.6, CF_3), 173.9, 176.9, 179.2. HRMS: $C_{21}H_{23}F_3O_{13}S$ requires M + 1 at m/z 573.0890; found, 573.0872.

7α-*O*-Acetate Ginkgolide B (4). Sodium acetate (163 mg, 1.99 mmol) and **3** (228 mg, 0.39 mmol) were dissolved in DMSO (3 mL), and the solution was stirred at 65 °C for 17 h. The solvent was removed in vacuo, and the residue was partitioned between 1 N HCl (20 mL) and EtOAc (25 mL). The aqueous phase was extracted with EtOAc (3 × 25 mL), the combined organic phases were washed with brine (2 × 10 mL) and dried ($MgSO_4$), and the solvent was removed in vacuo. The crude product was purified by flash chromatography eluting with $CHCl_3$/EtOAc/MeOH (10:1:1) to obtain **4** as white crystals (144 mg, 75%). A portion (20 mg) of this was recrystallized (MeOH/H_2O) for pharmacological evaluation (9 mg). ^{1}H NMR (400 MHz, DMSO-d_6): δ 1.12 (d, J = 7.1, CH_3), 1.10 (s, *tert*-butyl), 1.91 (d, J = 3.3, 8-H), 2.06 (s, $COCH_3$), 2.84 (q, J = 7.1, 14-H), 4.03 (dd, J = 7.7, 3.6, 1-H), 4.66 (d, J = 7.7, 2-H), 4.86 (d, J = 3.6, 1-OH), 5.01 (s, 6-H), 5.15 (d, J = 6.8, 10-H), 5.25 (d, J = 3.3, 7-H), 6.16 (s, 12-H), 6.52 (s, 3-OH), 7.42 (d, J = 6.8, 10-OH). ^{13}C NMR (100 MHz, CD_3OD): δ 8.0, 21.0, 30.7 (3C), 33.8, 43.4, 53.2, 70.1, 70.3, 72.5, 75.3, 79.6, 80.9, 84.6, 92.6, 99.8, 112.7, 171.3, 171.5, 175.0, 178.1. HPLC−UV: 96%. HRMS: $C_{22}H_{27}O_{12}$ requires M + 1 at m/z 483.1503; found, 483.1525.

7α-*O*-Phenylacetate Ginkgolide B (5). Sodium phenylacetate (44 mg, 0.28 mmol) and **3** (32 mg, 0.07 mmol) were dissolved in DMSO (0.8 mL) and heated at 65 °C for 5 h, the solvent was removed in vacuo, the residue was partitioned between 1 N HCl (10 mL) and EtOAc (15 mL), and the aqueous phase was extracted with EtOAc (3 × 15 mL). The combined organic phases were washed with 1 N HCl (2 × 10 mL), water (5 × 10 mL), and brine (2 × 10 mL) and dried ($MgSO_4$), and the solvent was removed in vacuo. The crude product was purified by flash column chromatography eluting with $CHCl_3$/MeOH/EtOAc (30:1:1), recrystallized (MeOH), and further purified by preparative HPLC (eluent A) to give **5** (10 mg, 26%) as white crystals. ^{1}H NMR (400 MHz, DMSO-d_6): δ 1.07 (s, *tert*-butyl), 1.12 (d, J = 6.9, CH_3), 1.93 (d, J = 2.9, 8-H), 2.84 (q, J = 6.9, 14-H), 3.70 (s, CH_2), 4.04 (dd, J = 3.6, 7.7, 1-H), 4.62 (d, J = 7.7, 2-H), 4.72 (d, J = 3.6, 1-OH), 4.99 (s, 6-H), 5.16 (d, J = 6.6, 10-H), 5.26 (d, J = 2.9, 7-H), 6.16 (s, 12-H), 6.48 (s, 3-OH), 7.25−7.35 (m, aromatic, 5H) 7.46 (d, J = 6.6, 10-OH). ^{13}C NMR (100 MHz, CD_3OD): δ 8.0, 30.8 (3C), 33.8, 42.2, 43.4, 53.3, 70.1, 70.3, 72.5, 75.2, 80.2, 81.0, 84.6, 92.6, 99.9, 112.7, 128.4, 129.7, 130.5, 134.7, 171.4, 172.2, 175.0, 178.1. HPLC−UV: 98%. HRMS: $C_{28}H_{31}O_{12}$ requires M + H at m/z 559.1816; found, 559.1826.

7α-Azido Ginkgolide B (6). Sodium azide (87 mg, 1.34 mmol) and **3** (153 mg, 0.27 mmol) were dissolved in DMSO (2.5 mL), and the solution was heated at 65 °C for 26 h. The solvent was removed in vacuo. The solid was partitioned between saturated aqueous NH_4Cl (20 mL) and EtOAc (20 mL), and the aqueous phase was extracted with EtOAc (3 × 20 mL). The combined organic phases were washed with brine (2 × 10 mL) and dried ($MgSO_4$), and the solvent was removed in vacuo. The crude product was purified by flash chromatography eluting with $CHCl_3$/MeOH/EtOAc (30:1:1) to give the **6** as white crystals (109 mg, 88%). A portion (23 mg) of this was recrystallized (MeOH/H_2O) for pharmacological evaluation (12 mg). ^{1}H NMR (300 MHz, DMSO-d_6): δ 1.12 (d, J = 7.1, CH_3), 1.13 (s, *tert*-butyl), 1.80 (d, J = 4.0, 8-H), 2.73 (q, J = 7.1, 14-H), 4.05 (dd, J = 7.6, 3.6, 1-H), 4.70 (d, J = 7.6, 2-H), 4.74 (d, J = 4.0, 7-H), 4.97 (d, J = 3.6, 1-OH), 5.06 (d, J = 6.0, 10-H), 5.25 (s, 6-H), 6.10 (s, 12-H), 6.52 (s, 3-OH), 7.05 (d, J = 6.0, 10-OH). ^{13}C NMR (100 MHz, DMSO-d_6): δ 7.8, 30.1 (3C), 32.7, 41.6, 51.6, 67.2, 68.4, 68.5, 71.0, 73.7, 79.6, 82.9, 92.9, 98.2, 110.3, 169.5, 173.4, 176.2. HPLC−UV: 99%. HRMS: $C_{20}H_{24}O_{10}N_3$ requires M + 1 at m/z 466.1462; found, 466.1445.

7α-Fluoro Ginkgolide B (7). Tetrabutylammonium fluoride hydrate (37 mg, 0.14 mmol) and **3** (62 mg, 0.11 mmol) were dissolved in CH_3CN (1 mL) and heated at 80 °C for 1.5 h. The solvent was removed in vacuo, the residue was partitioned between 1 N HCl (10 mL) and EtOAc (15 mL), and the aqueous phase was extracted with EtOAc (3 × 15 mL). The combined organic phases were washed with water (2 × 15 mL) and brine (2 × 15 mL) and dried ($MgSO_4$), and the solvent was removed in vacuo. The crude product was purified by flash column chromatography eluting with $CHCl_3$/MeOH/EtOAc (30:1:1) followed by preparative HPLC (eluent B) to give **7** as white crystals (34 mg, 71%). ^{1}H NMR (400 MHz, CD_3OD): δ 1.25 (s, *tert*-butyl), 1.26 (d, J = 7.1, CH_3), 1.94 (dd, $^2J_{HF}$ = 45.5, J = 2.3, 8-H), 3.05 (q, J = 7.1, 14-H), 4.24 (d, J = 8.0, 1-H), 4.59 (d, J = 8.0, 2-H), 5.18 (s, 10-H), 5.35 (d, $^2J_{HF}$ = 10.9, 6-H), 5.38 (dd, $^1J_{HF}$ = 48.8, J = 2.3, 7-H), 6.14 (s, 12-H). ^{13}C NMR (75 MHz, CD_3OD): δ 7.0, 29.5 (3C), 32.9, 42.4, 53.7

($^2J_{CF}$ = 20.4 Hz), 68.8, 69.1, 71.5, 74.5, 79.5 ($^2J_{CF}$ = 36.0 Hz), 83.7, 91.7, 96.9 ($^1J_{CF}$ = 184.2 Hz), 98.8, 111.6, 171.2, 173.9, 177.1. HRMS: $C_{20}H_{23}FO_{10}$ requires M + 1 at *m/z* 443.1354; found, 443.1370.

7α-Chloro Ginkgolide B (8). Tetrabutylammonium chloride (86 mg, 0.31 mmol) and **3** (36 mg, 0.06 mmol) were dissolved in CH_3CN (1.4 mL) and heated at 80 °C for 12 h. The solvent was removed in vacuo, and the residue partitioned between 1 N HCl (20 mL) and EtOAc (20 mL). The aqueous phase was extracted with EtOAc (3 × 20 mL). The combined organic phases were washed with water (4 × 10 mL) and brine (2 × 10 mL) and dried ($MgSO_4$), and the solvent was removed in vacuo. The crude product was purified by preparative HPLC (eluent B) and recrystallized ($CH_3CN/CHCl_3$) to give **8** as white crystals (9 mg, 30%). ^{1}H NMR (400 MHz, DMSO-d_6): δ 1.12 (d, *J* = 7.0, CH_3), 1.17 (s, *tert*-butyl), 2.19 (d, *J* = 4.2, 8-H), 2.85 (q, *J* = 7.0, 14-H), 4.03 (dd, *J* = 7.7, 3.3, 1-H), 4.63 (d, *J* = 3.3, 1-OH), 4.68 (d, *J* = 7.8, 2-H), 4.84 (d, *J* = 4.2, 7-H), 5.13 (d, *J* = 6.4, 10-H), 5.26 (s, 6-H), 6.17 (s, 12-H), 6.53 (s, 3-OH), 7.57 (d, *J* = 6.4, 10-OH). ^{13}C NMR (100 MHz, CD3OD): δ 8.7, 31.2 (3C), 34.5, 42.5, 54.2, 65.1, 69.0, 70.0, 72.2, 74.4, 83.7, 84.2, 90.7, 99.4, 111.3, 169.9, 174.4, 177.1. HPLC–UV: 98%. HRMS: $C_{20}H_{24}O_{10}Cl$ requires M + 1 at *m/z* 459.1058; found, 459.1052.

Neoginkgolide C (9). Triflate **3** (27 mg, 0.05 mmol) was dissolved in dry MeOH (470 μL) and 2,6-lutidine (150 μL) was added, and the reaction mixture was heated at 65 °C for 3 days. The solvent was removed in vacuo and the residue purified by flash chromatography eluting with $CHCl_3$/MeOH/EtOAc (20:1:1) to give the crude product, which was further purified by preparative HPLC (eluent A) to give **9** as white crystals (6 mg, 29%). ^{1}H NMR (400 MHz, CD_3OD): δ 1.20 (m, CH_3 and *tert*-butyl), 1.64 (dd, *J* = 1.4, 1.2, 8-H), 3.72 (q, *J* = 7.1, 14-H), 4.46 (d, *J* = 8.0, 2-H), 4.59 (d, *J* = 1.2, 10-H), 4.72 (d, *J* = 8.0, 1-H), 5.00 (dd, *J* = 1.4, 1.3, 7-H), 5.14 (d, *J* = 1.3, 6-H), 5.96 (s, 12-H). ^{13}C NMR (100 MHz, DMSO-d_6): δ 7.6, 30.2 (3C), 32.7, 41.3, 47.8, 60.2, 66.9, 67.8, 73.6, 75.6, 82.5, 83.4, 92.7, 93.7, 104.9, 170.2, 171.7, 177.6. HPLC–UV: 98%. HRMS: $C_{20}H_{24}O_{11}$ requires M + Na at *m/z* 463.1216; found, 463.1245.

10-*O*-Acetate-7-trifluoromethanesulfonyloxy Ginkgolide B (10). Potassium thioacetate (4 mg, 0.035 mmol) and **3** (3 mg, 0.006 mmol) were dissolved in dry DMF (35 μL) and heated at 40 °C for 3 h. The solvent was removed in vacuo, and residue was partitioned between water (10 mL) and EtOAc (15 mL), and the aqueous phase was extracted with EtOAc (3 × 15 mL). The combined organic phases were washed with water (5 × 10 mL) and brine (2 × 10 mL) and dried ($MgSO_4$), and the solvent was removed in vacuo. The crude product was purified by flash chromatography eluting with $CHCl_3$/MeOH/EtOAc (20:1:1) to give **10** (1.3 mg, 18%) as white crystals. ^{1}H NMR (400 MHz, DMSO-d_6): δ 1.08 (s, *tert*-butyl), 1.13 (d, *J* = 7.1, CH_3), 2.21 (s, $COCH_3$), 2.31 (d, *J* = 12.6, 8-H), 2.85 (q, *J* = 7.1, 14-H), 4.08 (dd, *J* = 5.9, 5.8, 1-H), 4.75 (d, *J* = 5.9, 2-H), 5.09 (dd, *J* = 12.6, 4.2, 7-H), 5.48 (d, *J* = 4.2, 6-H), 6.13 (s, 10-H), 6.33 (s, 12-H), 6.53 (s, 3-OH), 6.71 (d, *J* = 5.8, 1-OH). HRMS: $C_{23}H_{26}O_{14}F_3S$ requires M + 1 at *m/z* 615.0995; found, 615.1016.

7α-*N*-Methylamino Ginkgolide B (11). Azide **6** (38 mg, 0.08 mmol) was dissolved in dry MeOH (1.2 mL), and Pd/C (10%, 12 mg) was added. The suspension was stirred under an atmosphere of H_2 for 48 h. The solvent was removed in vacuo, EtOAc (10 mL) was added, and the solution was filtered through Celite. The solvent was removed in vacuo, and the crude product was purified by flash chromatography eluting with $CHCl_3$/MeOH/EtOAc (30:1:1) to give white crystals, which were recrystallized (MeOH) to give **11** (23 mg, 65%) as white crystals. ^{1}H NMR (400 MHz, CD_3OD): δ 1.22 (m, *tert*-butyl and CH_3), 1.89 (d, *J* = 4.4, 8-H), 2.47 (s, CH_3), 3.06 (q, *J* = 7.0, 14-H), 3.46 (d, *J* = 4.4, 7-H), 4.24 (d, *J* = 7.2, 1-H), 4.53 (d, *J* = 7.2, 2-H), 5.05 (s, 6-H), 5.31 (s, 10-H), 6.17 (s, 12-H). ^{13}C NMR (100 MHz, CD_3OD): δ 8.2, 31.3 (3C), 33.4, 34.3, 43.3, 53.5, 69.1, 69.6, 70.8, 72.6, 75.4, 79.3, 84.4, 94.5, 100.6, 112.2, 172.6, 174.8, 178.4. HPLC–UV: 97%. HRMS: $C_{21}H_{28}O_{10}N$ requires M + 1 at *m/z* 454.1713; found, 454.1719.

7α-*N*-Ethylamino Ginkgolide B (12). Azide **6** (48 mg, 0.10 mmol) was dissolved in dry EtOH (1.0 mL), and Pd/C (10%, 15 mg) was added. The suspension was stirred under an atmosphere of H_2 for 48 h. The solvent was removed in vacuo, EtOAc (10 mL) was added, and the solution was filtered through Celite. The solvent was removed in vacuo and the residue purified by flash chromatography eluting with $CHCl_3$/MeOH/EtOAc (30:1:1) to give white crystals, which were recrystallized (MeOH) to give **12** (22 mg, 47%). ^{1}H NMR (300 MHz, CD_3OD): δ 1.11 (t, *J* = 7.1, CH_3), 1.23 (m, *tert*-butyl and CH_3), 1.89 (d, *J* = 4.5, 8-H), 2.57 (dq, *J* = 7.1, 12.0, CH_2, 1H), 2.94 (dq, *J* = 7.1, 12.0, CH_2, 1H), 3.06 (q, *J* = 7.1, 14-H), 3.56 (d, *J* = 4.5, 7-H), 4.22 (d, *J* = 7.3, 1-H), 4.53 (d, *J* = 7.3, 2-H), 5.08 (s, 6-H), 5.27 (s, 10-H), 6.16 (s, 12-H). ^{13}C NMR (100 MHz, CD_3OD): δ 8.2, 15.5, 31.3 (3C), 34.4, 41.6, 43.3, 53.5, 67.5, 69.2, 70.8, 72.6, 75.3, 80.0, 84.4, 94.4, 100.6, 112.3, 172.6, 174.9, 178.4. HPLC–UV: 98%. HRMS: $C_{22}H_{29}O_{10}N$ requires M + 1 at *m/z* 468.1870; found, 468.1867.

7α-Amino Ginkgolide B (13). Azide **6** (10 mg, 0.02 mmol) was dissolved in dry THF (0.4 mL), and Pd/C (10%, 8 mg) was added. The suspension was stirred under an atmosphere of H_2 for 14 h. EtOAc (10 mL) was added and the solution filtered through Celite. The solvent was removed in vacuo to give white crystals which were recrystallized (MeOH) to give **13** as white crystals (5 mg, 49%). ^{1}H NMR (400 MHz, CD_3OD): δ 1.20 (s, *tert*-butyl), 1.23 (d, *J* = 7.1, CH_3), 1.90 (d, *J* = 3.2, 8-H), 3.08 (q, *J* = 7.1, 14-H), 3.83 (d, *J* = 3.2, 7-H), 4.26 (d, *J* = 7.0, 1-H), 4.51 (d, *J* = 7.0, 2-H), 5.01 (s, 6-H), 5.04 (s, 10-H), 6.18 (s, 12-H). ^{13}C NMR (100 MHz, CD_3OD): δ 8.3, 31.0 (3C), 34.1, 43.2, 54.7, 60.3, 68.9, 70.9, 72.6, 74.9, 83.9, 84.4, 95.0, 100.3, 111.8, 172.3, 174.4, 178.4. HPLC–UV: 97%. HRMS: $C_{42}H_{26}O_{10}N$ requires M + H at *m/z* 440.1557; found, 440.1594.

7-Epi-ginkgolide C (14). Acetate **4** (42 mg, 0.087 mmol) was dissolved in a mixture of MeOH and 2 N NaOH (2:1, 1.8 mL) and stirred for 5 h. HCl (1 N) was added, and the aqueous phase was extracted with EtOAc (3 ×20 mL). The combined organic phases were washed with brine (2 × 10 mL) and dried ($MgSO_4$), and the solvent was removed in vacuo to give **14** (36 mg, 95%) as white crystals. A portion (15 mg) of this was recrystallized (MeOH/H_2O) for pharmacological evaluation (6 mg). ^{1}H NMR (400 MHz, DMSO-d_6): δ 1.12 (d, *J* = 7.0, CH_3), 1.12 (s, *tert*-butyl), 1.64 (d, *J* = 2.7, 8-H), 2.89 (q, *J* = 7.0, 14-H), 4.11 (dd, *J* = 4.5, 6.8, 1-H), 4.37 (dd, *J* = 2.7, 6.3, 7-H), 4.59 (d, *J* = 6.8, 2-H), 4.98 (s, 6-H), 5.04 (d, *J* = 2.7, 10-H), 5.52 (d, *J* = 6.3, 7-OH), 5.64 (d, *J* = 4.5, 1-OH), 6.13 (s, 12-H), 6.45 (s, 3-OH), 6.73 (d, *J* = 2.7, 10-OH). ^{13}C NMR (75 MHz, DMSO-d_6): δ 8.0, 30.2 (3C), 32.6, 41.4, 52.3, 68.8, 69.6, 71.5, 73.4, 76.2, 80.8, 82.8, 92.9, 98.6, 109.7, 170.0, 172.7, 176.3. HPLC–UV: 98%. HRMS: $C_{20}H_{25}O_{11}$ requires M + 1 at *m/z* 441.1397; found, 441.1395.

10-*O*-Benzyl Ginkgolide B (15). Synthesis and analytical data as previously described.[19,21]

10-*O*-Benzyl Ginkgolide C (16). K_2CO_3 (31 mg, 0.22 mmol) was added to a solution of **2** (12 mg, 0.02 mmol) dissolved in DMF (0.2 mL) followed by addition of benzyl chloride (30 μL, 0.26 mmol). The suspension was stirred for 2.5 h at 60 °C. The solvent was removed in vacuo, the residue was partitioned between 1 N HCl (10 mL) and EtOAc (15 mL), and the aqueous phase was extracted with EtOAc (3 × 15 mL). The combined organic phases were washed with water (2 × 10 mL) and brine NaCl (2 × 10 mL) and dried ($MgSO_4$), and the solvent was removed in vacuo. The crude product was purified by flash chromatography eluting with $CHCl_3$/MeOH/EtOAc (20:1:1) and further by preparative HPLC (solvent system A) to give **16** (9 mg, 77%) as white crystals. ^{1}H NMR (400 MHz, CD_3OD): δ 1.21 (s, *tert*-butyl), 1.23 (d, *J* = 7.1, CH_3), 1.76 (d, *J* = 12.5, 8-H), 3.01 (q, *J* = 7.1, 14-H), 4.13 (dd, *J* = 12.3, 4.3, 7-H), 4.19 (d, *J* = 7.4, 1-H), 4.49 (d, *J* = 7.4, 2-H), 4.76 (d, *J* = 10,2, CH_2, 1H), 5.04 (s, 6-H), 5.02 (d, *J* = 4.3, 6-H), 5.25 (s, 10-H), 5.46 (d, *J* = 10.2, CH_2, 1H), 6.14 (s, 12-H), 7.37–7.44 (m, aromatic, 5H). ^{13}C NMR (75 MHz, $CDCl_3$): δ 7.2, 29.1 (3C), 32.2, 41.6, 50.5, 64.1, 67.1, 73.8, 74.3, 75.6,

77.2, 79.3, 83.5, 90.6, 98.5, 110.1, 128.9 (2C), 129.5 (2C), 129.8, 134.2, 170.8, 170.8, 175.5. HPLC–UV: 98%. HRMS: $C_{27}H_{30}O_{11}$ requires M + Na at *m/z* 553.1686; found, 553.1684.

10-*O*-Benzyl-7α-fluoro Ginkgolide B (17). Synthesized as described for **16** using K_2CO_3 (107 mg, 0.77 mmol), **7** (34 mg, 0.08 mmol), and benzyl chloride (89 μL, 0.77 mmol) in DMF (1.8 mL). The crude product was purified by flash chromatography eluting with $CHCl_3$/MeOH/EtOAc (30:1:1) to give **17** (16 mg, 39%) as white crystals. ^{1}H NMR (400 MHz, $CDCl_3$): δ 1.25 (s, *tert*-butyl), 1.30 (d, J = 7.0, CH3), 1.88 (dd, $^2J_{HF}$ = 44.5, J = 2.3, 8-H), 2.94 (d, J = 3.1, 1-OH), 3.06 (q, J = 7.0, 14-H), 4.28 (dd, J = 8.1, 3.1, 1-H), 4.50 (d, J = 8.1, 2-H), 4.68 (d, J = 9.4, CH_2, 1H), 4.95 (s, 10-H), 5.29 (d, $^2J_{HF}$ = 10.2, 6-H), 5.30 (dd, $^1J_{HF}$ = 50.1, J = 1.5, 7-H), 5.41 (d, J = 9.4, CH_2, 1H), 6.04 (s, 12-H), 7.36 (m, aromatic, 5H). ^{13}C NMR (100 MHz, $CDCl_3$): δ 7.2, 30.3 (3C), 32.9, 41.7, 53.3 ($^2J_{CF}$ = 20.4), 68.2, 71.6, 74.1, 74.4, 75.1, 79.5 ($^2J_{CF}$ = 35.6), 83.6, 90.2, 96.0 ($^1J_{CF}$ = 184.2), 98.2, 110.9, 128.7 (2C), 129.1 (2C), 129.3, 134.8, 170.2, 170.8, 175.1. HPLC–UV: 98%. HRMS: $C_{27}H_{30}O_{10}F$ requires M + 1 at *m/z* 533.1823; found, 533.1784.

10-*O*-Benzyl-7-epi-ginkgolide C (18). Synthesized as described for **16** using K_2CO_3 (50 mg, 0.36 mmol), **14** (16 mg, 0.04 mmol), and benzyl chloride (42 μL, 0.36 mmol) in DMF (0.3 mL). The crude product was purified by flash chromatography eluting with $CHCl_3$/MeOH/EtOAc (20:1:1) and further by preparative HPLC (eluent A) to give **18** (11 mg, 56%) as white crystals. ^{1}H NMR (400 MHz, $CDCl_3$): δ 1.23 (s, *tert*-butyl), 1.29 (d, J = 7.0, CH_3), 1.83 (d, J = 3.1, 8-H), 2.60 (d, J = 3.6, 1-OH), 2.66 (d, J = 11.0, 7-OH), 3.06 (q, J = 7.0, 14-H), 3.40 (bs, 3-OH), 4.28 (dd, J = 3.6, 7.8, 1-H), 4.48 (m, 2-H, 7-H), 4.72 (d, J = 9.2, CH_2, 1H), 4.96 (s, 6-H), 5.51 (s, 10-H), 5.50 (d, J = 9.2, CH_2, 1H), 6.09 (s, 12-H), 7.39–7.44 (m, aromatic, 5H). ^{13}C NMR (100 MHz, $CDCl_3$): δ 7.3, 30.6 (3C), 33.1, 41.6, 52.9, 68.4, 71.3, 74.0, 74.4, 74.7, 77.6, 82.3, 83.2, 90.7, 98.5, 110.5, 129.2 (2C), 129.6 (2C), 130.1, 133.8, 170.3, 170.5, 175.4. HPLC–UV: 99%. HRMS: $C_{27}H_{31}O_{11}$ requires M + 1 at *m/z* 531.1866; found, 531.1895.

Radioligand Binding Assay. The radioligand binding assays were performed as previously described.[30] In brief, membrane fractions from hearts and skeletal muscles of PAFR-Transgenic mice (50 μL suspension containing 158 fmol of PAFR) were mixed with 2 pmol of [^{3}H]-WEB 2086 in 50 μL of buffer [25 mM HEPES/NaOH (pH 7.4), 0.25 M sucrose, 10 mM $MgCl_2$, 0.1% BSA] and the compound to be tested in 100 μL of buffer in a 96-well microplate in triplicate for each concentration. These mixtures were incubated at 25 °C for 90 min, upon which the receptor-bound [^{3}H]-WEB 2086 was filtered and washed with cold buffer. The filters were then dried at 50 °C for at least 90 min, 25 μL of MicroScint-0 scintillation cocktail was added, and filters were placed in a TopCount microplate scintillation counter. Binding data were analyzed with the nonlinear curve-fitting program Microplate Manager III (Bio-Rad, Hercules, CA). Nonspecific binding was determined using methods as previously described.[30]

Acknowledgment. We are grateful to Dr. Yasuhiro Itagaki for performing HRMS and Dr. Nasri Nesnas for discussions. We thank the following for financial support: Memory Pharmaceuticals Corp., the Alfred Benzon Foundation (to K.S.), the Welfide Medicinal Research Foundation (to H.S.), the Alfred Bader Foundation (to S.J.), and the Ministry of Health, Labor and Welfare, Japan (to S.I.) for a Grants-in-Aid for Comprehensive Research on Aging and Health and Research on Allergic Disease and Immunology.

Supporting Information Available: COSY, HSQC, and ROESY spectra of compound **9**. This material is available free of charge via the Internet at http://pubs.acs.org.

References

(1) Drieu, K.; Jaggy, H. History, development and constituents of EGb 761. In *Medicinal and Aromatic Plants-Industrial Profiles: Ginkgo biloba*, van Beek, T. A., Ed.; Harwood Academic Publishers: Amsterdam, 2000; Vol. 12, pp 267–277.
(2) DeFeudis, F. V.; Drieu, K. Ginkgo biloba extract (EGb 761) and CNS functions: basic studies and clinical applications *Curr. Drug Targets* **2000**, *1*, 25–58.
(3) DeFeudis, F. V. *Ginkgo biloba extract (EGb 761). From chemistry to clinic*; Ullstein Medical: Wiesbaden, 1998; p 401.
(4) Oken, B. S.; Storzbach, D. M.; Kaye, J. A. The efficacy of Ginkgo biloba on cognitive function in Alzheimer disease. *Arch. Neurol.* **1998**, *55*, 1409–1415.
(5) Diamond, B. J.; Shiflett, S. C.; Feiwel, N.; Mathies, R. J.; Noskin, O.; Richards, J. A.; Schoenberger, N. E. Ginkgo biloba extract: mechanisms and clinical indications. *Arch. Phys. Med. Rehabil.* **2000**, *81*, 668–678.
(6) van Dongen, M. C. J. M.; van Rossum, E.; Knipschild P. Efficacy of Ginkgo biloba special extracts – evidence from randomized clinical trials. In *Medicinal and Aromatic Plants-Industrial Profiles: Ginkgo biloba*; van Beek, T. A., Ed.; Harwood Academic Publishers: Amsterdam, 2000; Vol. 12, pp 385–442.
(7) Kennedy, D. O.; Scholey, A. B.; Wesnes, K. A. The dose-dependent cognitive effects of acute administration of Ginkgo biloba to healthy young volunteers. *Psychopharmacology* **2000**, *151*, 416–423.
(8) Polich, J.; Gloria, R. Cognitive effects of a Ginkgo biloba/vinpocetine compound in normal adults: systematic assessment of perception, attention and memory. *Hum. Psychopharmacol. Clin. Exp.* **2001**, *16*, 409–416.
(9) Nakanishi, K. The ginkgolides. *Pure Appl. Chem.* **1967**, *14*, 89–113 and references therein.
(10) Okabe, K.; Yamada, K.; Yamamura, S.; Takada, S. Ginkgolides. *J. Chem. Soc. C* **1967**, 2201–2206.
(11) Nakanishi, K.; Habaguchi, K.; Nakadaira, Y.; Woods, M. C.; Maruyama, M.; Major, R. T.; Alauddin, M.; Patel, A. R.; Weinges, K.; Bähr, W. Structure of bilobalide, a rare *tert*-butyl containing sesquiterpenoid related to the C_{20}-ginkgolides. *J. Am. Chem. Soc.* **1971**, *93*, 3544–3546.
(12) Weinges, K.; Hepp, M.; Jaggy, H. Chemie der Ginkgolide, II. Isolierung und Strukturaufklärung eines neuen Ginkgolids *Liebigs Ann. Chem.* **1987**, 521–526.
(13) Braquet, P. The ginkgolides: potent platelet-activating factor antagonists isolated from Ginkgo biloba L.: chemistry, pharmacology and clinical applications. *Drugs Future* **1987**, *12*, 643–699.
(14) Braquet, P. Esanu, A.; Buisine, E.; Hosford, D.; Broquet, C.; Koltai, M. Recent progress in ginkgolide research. *Med. Chem. Rev.* **1991**, *11*, 295–355.
(15) Singh, M.; Saraf, M. K. Platelet-activating factor: a new target site for the development of nootropic agents. *Drugs Future* **2001**, *26*, 883–888.
(16) Kato, K.; Clark, G. D.; Bazan, N. G.; Zorumski, C. F. Platelet-activating factor as a potential retrograde messenger in CA1 hippocampal long-term potentiation. *Nature* **1994**, *367*, 175–179.
(17) Corey, E. J.; Gavai, A. V. Simple analogues of ginkgolide B which are highly active antagonists of platelet activating factor. *Tetrahedron Lett.* **1989**, *30*, 6959–6962.
(18) Corey, E. J.; Rao, K. S. Enantioselective total synthesis of ginkgolide derivatives lacking the *tert*-butyl group, an essential structural subunit for antagonism of platelet activating factor. *Tetrahedron Lett.* **1991**, *32*, 4623–4626.
(19) Park, P.-U.; Pyo, S.; Lee, S.-K.; Sung, J. H.; Kwak, W. J.; Park, H.-K.; Cho, Y.-B.; Ryu, G. H.; Kim, T. S. Ginkgolide derivatives. U.S. Patent 5,541,183, 1996.
(20) Hu, L.; Chen, Z.; Cheng, X.; Xie, Y. Chemistry of ginkgolides: structure–activity relationship as PAF antagonists. *Pure Appl. Chem.* **1999**, *71*, 1153–1156.
(21) Hu, L.; Chen, Z.; Xie, Y.; Jiang, H.; Zhen, H. Alkyl and alkoxycarbonyl derivatives of ginkgolide B: synthesis and biological evaluation of PAF inhibitory activity. *Bioorg. Med. Chem.* **2000**, *8*, 1515–1521.
(22) Strømgaard, K.; Saito, D. R.; Shindou, H.; Ishii, S.; Shimizu, T.; Nakanishi, K. Ginkgolide derivatives for photolabeling studies: preparation and pharmacological evaluation. *J. Med. Chem.* **2002**, *45*, 4038–4046.
(23) Pietri, S.; Liebgott, T.; Finet, J.-P.; Culcasi, M.; Billottet, L.; Bernard-Henriet, C. Synthesis and biological studies of a new ginkgolide C derivative: evidence that the cardioprotective effect of ginkgolides is unrelated to PAF inhibition. *Drug. Dev. Res.* **2001**, *54*, 191–201.
(24) Suehiro, M.; Strømgaard, K.; Nakanishi, K. Unpublished results.
(25) Smart, B. E. Fluorine substituent effects (on bioactivity) *J. Fluorine Chem.* **2001**, *109*, 3–11.
(26) Teng, B.-P. Preparation process of ginkgolide B from ginkgolide C. U.S. Patent 5,599,950, 1997.
(27) Jaracz, S.; Strømgaard, K.; Nakanishi, K. Ginkgolides: selective acetylations, translactonization and biological evaluation. *J. Org. Chem.* **2002**, *67*, 4623–4626.
(28) Hu, L.; Chen, Z.; Xie, Y. Synthesis and biological activity of amide derivatives of ginkgolide A. J. *Asian Nat. Prod. Res.* **2001**, *3*, 219–227.

(29) Moriarty, R. M.; Zhuang, H.; Penmasta, R.; Liu, K.; Awasthi, A. K.; Tuladhar, S. M.; Rao, M. S. C.; Singh, V. K. Inversion of configuration of α-trisubstituted (neopentyl) type secondary alcohols. *Tetrahedron Lett.* **1993**, *34*, 8029−8032.
(30) Shindou, H.; Ishii, S.; Uozumi, N.; Shimizu, T. Roles of cytosolic phopholipase A2 and platelet-activating factor receptor in the Ca-induced biosynthesis of PAF. *Biochem. Biophys. Res. Commun.* **2000**, *271*, 812−817.
(31) Lichtblau, D.; Berger, J. M.; Nakanishi, K. An efficient extraction of ginkgolides and bilobalide from Ginkgo biloba leaves. *J. Nat. Prod.* **2002**, *65*, 1501−1504.
(32) van Beek, T. A.; Lelyved, G. P. Preparative isolation and separation procedure for ginkgolides A, B, C, and J and bilobalide. *J. Nat. Prod.* **1997**, *60*, 735−738.

JM0203985

European Journal of Neuroscience, Vol. 18, pp. 563–570, 2003

Involvement of platelet-activating factor and LIS1 in neuronal migration

Suzumi M. Tokuoka,[1] Satoshi Ishii,[1] Noriko Kawamura,[2] Mamoru Satoh,[2] Atsuyoshi Shimada,[2] Shinji Sasaki,[3] Shinji Hirotsune,[3,4] Anthony Wynshaw-Boris[5] and Takao Shimizu[1]

[1]Department of Biochemistry and Molecular Biology, Faculty of Medicine, The University of Tokyo, CREST of JST, Tokyo 113–0033, Japan

[2]Department of Pathology, Institute for Developmental Research Aichi Human Service Center, CREST of JST, Aichi 480–0392, Japan

[3]Center for Genome Medical Science, Saitama Medical School, Saitama 350–1241, Japan

[4]PRESTO of JST, Japan

[5]Departments of Pediatrics and Medicine, University of California San Diego, School of Medicine, La Jolla, California 92093–0627, USA

Keywords: cerebellar granule cell, knockout mouse, lissencephaly, PAF acetylhydrolase, PAF receptor

Abstract

Platelet-activating factor (PAF, 1-*O*-alkyl-2-acetyl-*sn*-glycero-3-phosphocholine) is a biologically active lipid mediator. We have previously shown the expression of PAF receptor in neurons and microglia. PAF is produced in the brain from its precursor, and degraded by the enzyme PAF acetylhydrolase. LIS1 is a regulatory subunit of PAF acetylhydrolase, and is identical to a gene whose deletion causes the human neuronal migration disorder, type I lissencephaly. Indeed, *Lis1* mutant mice display defects in neuronal migration and layering *in vivo*, and also in cerebellar granule cell migration *in vitro*. However, the roles of PAF and the PAF receptor in the neuronal migration remain to be determined. Here, we show that PAF receptor-deficient mice exhibited histological abnormalities in the embryonic cerebellum. PAF receptor-deficient cerebellar granule neurons migrated more slowly *in vitro* than wild-type neurons, consistent with the observation that a PAF receptor antagonist reduced the migration of wild-type neurons *in vitro*. Synergistic reduction of neuronal migration was observed in a double mutant of PAF receptor and LIS1. Unexpectedly, PAF affected the migration of PAF receptor-deficient neurons, suggesting a receptor-independent pathway for PAF action. The PAF receptor-independent response to PAF was abolished in granule neurons derived from the double mutant mice. Thus, our results suggest that the migration of cerebellar granule cells is regulated by PAF through receptor-dependent and receptor-independent pathways, and that LIS1 is a pivotal molecule that links PAF action and neuronal cell migration both *in vivo* and *in vitro*.

Introduction

Platelet-activating factor (PAF, 1-*O*-alkyl-2-acetyl-*sn*-glycero-3-phosphocholine) is a potent lipid mediator that has biological effects on a variety of cells and tissues (Ishii & Shimizu, 2000; Prescott *et al.*, 2000; Honda *et al.*, 2002). PAF acts by binding to a G-protein-coupled seven transmembrane receptor (Honda *et al.*, 1991; Nakamura *et al.*, 1991) which activates several second messenger systems (Ishii & Shimizu, 2000; Prescott *et al.*, 2000; Honda *et al.*, 2002). We generated PAF receptor-deficient (*Pafr−/−*) mice by homologous recombination (Ishii *et al.*, 1998b). Using these mice we have shown that PAF is involved in various physiological and pathological processes (Nagase *et al.*, 1999; Wu *et al.*, 2001; Nagase *et al.*, 2002).

Expression of PAF receptor in brain has been demonstrated by radioligand binding assay (Marcheselli *et al.*, 1990; Bito *et al.*, 1992), and Northern blotting and *in situ* hybridization in rats and mice (Bito *et al.*, 1992; Ishii *et al.*, 1996; Mori *et al.*, 1996). Although PAF synthesizing enzymes have not yet been characterized completely (Snyder, 1995; Henneberry *et al.*, 2000), production of PAF in the mammalian brain has been reported (Yue *et al.*, 1990; Baker, 1995). PAF enhances excitatory synaptic transmission (Clark *et al.*, 1992; Kato *et al.*, 1994; Grassi *et al.*, 1998; Chen *et al.*, 2001). PAF seems to mediate the neurotoxic effect of glutamate on neuronal cells (DeCoster *et al.*, 1998; Ogden *et al.*, 1998). PAF was produced from HIV-infected monocytes in brain and induces neuronal apoptosis (Gelbard *et al.*, 1994; Talley *et al.*, 1995). PAF receptor antagonists suppress ischemic brain injury (Lindsberg *et al.*, 1991; Yue & Feuerstein, 1994). *Ginkgo biloba* extracts, which exhibit therapeutic activity in a variety of disorders including Alzheimer's disease, act as PAF receptor antagonists (Kanowski *et al.*, 1996; Strømgaard *et al.*, 2002).

Lis1 was identified as the gene mutated in a severe human developmental brain malformation known as lissencephaly type I (Reiner *et al.*, 1993). PAF acetylhydrolase, an inactivating enzyme for PAF (Hattori *et al.*, 1993; Hattori *et al.*, 1994b), was purified, and one of the trimeric subunits is completely identical to LIS1. LIS1 interacts with two catalytic subunits of PAF acetylhydrolase, but LIS1 itself does not have an enzymatic activity (Hattori *et al.*, 1994a; Hattori *et al.*, 1995). Mouse embryos with homozygous deletions of *Lis1* gene die soon after implantation, while heterozygous *Lis1* mutant mice display defects in neuronal migration and layering *in vivo*, and also in cerebellar granule cell migration *in vitro* (Hirotsune *et al.*, 1998; Cahana *et al.*, 2001).

Correspondence: Dr Takao Shimizu, as above.
E-mail: tshimizu@m.u-tokyo.ac.jp

Received 27 December 2002, revised 21 April 2003, accepted 15 May 2003

doi:10.1046/j.1460-9568.2003.02778.x

Recent studies have identified several molecules that interact with the LIS1 protein, and have suggested that LIS1 regulates dynein motor function and microtubule organization (Morris, 2000; Wynshaw-Boris & Gambello, 2001).

We explored the role of PAF receptor in neuronal migration, using *Pafr−/−* mice. Our data demonstrate histological abnormalities in embryonic mouse brain and an impairment of *in vitro* neuronal migration in the PAF receptor-deficient mice. Thus, we propose that the PAF–PAF receptor pathway may have a significant effect on neuronal migration and development at the embryonic stage.

Materials and methods

Mice

The generation of *Pafr−/−* mice and *Lis1* heterozygous (*Lis1+/−*) mice has been described previously (Hirotsune *et al.*, 1998; Ishii *et al.*, 1998b). *Pafr−/−* mice had been backcrossed to wild-type C57BL/6 mice seven times (F7) for cerebellar granule cell culture and nine times (F9) for histologic evaluations. *Lis1+/−* mice on the 129SvEv × NIH Black Swiss mixed genetic background (Hirotsune *et al.*, 1998) were mated to *Pafr−/−* or *Pafr+/−* mice from F9 or F10 generations on C57BL/6 background up to six or seven times. We used littermates of *Pafr+/−Lis1+/−*, *Pafr−/−Lis1+/−* and *Pafr+/−Lis1+/+* mice produced by mating *Pafr−/−Lis1+/−* females and *Pafr+/−* males. Adult/post-natal and embryonic animals were killed by cervical dislocation and decapitation, respectively.

Histology

The brains were fixed with formalin and embedded in paraffin. Serial sections were made of 8-μm thickness and stained with haematoxylin and eosin. Coronal sections were made from mice at E17.5. Serial sections were made and measured on the sections cut at the level through the aqueduct and the inferior colliculus dorsally, and the fourth ventricle and medulla oblongata ventrally. Two parts of the external granular layer (EGL) were set for the measurements as indicated in Fig. 1A, one on the midline and the other at 300 μm lateral to the midline. For E14.5 mice, parasagittal sections were made and the area of interest for the measurements was set on the section cut approximately at 200 μm lateral to the midline. This part of the EGL was located at the dorsal surface of the cerebellar primordium and near the leading edge of the EGL in both wild-type and *Pafr−/−* mice. When the thickness of the EGL was measured in each specimen, an 80-μm-long segment of the EGL in the area of interest was selected as described in Fig. 1B and C. The thickness of the layer was measured at five points 20 μm apart from each other in the 80-μm-long segments and the mean values were taken. These measurements were performed in a blinded manner.

Granule cell reaggregate cultures

Cerebellar granule cell reaggregates were cultured as described previously (Asou *et al.*, 1992; Adachi *et al.*, 1997; Bix & Clark, 1998) with some modifications as follows. Cerebella were obtained from P2–P4 mice and digested with 1.0 mg/mL dispase (Invitrogen, Grand Island, NY, USA) in Dulbecco's modified Eagle's medium (DMEM) with high glucose (Invitrogen), containing 15 mM Hepes/NaOH (pH 7.4), for 15 min at 30 °C. The tissues were then triturated through fire-polished Pasteur pipettes in 4 mL of DMEM containing 0.5 mg/mL DNase I (Roche Diagnostics, Mannheim, Germany). After standing for 5 min on ice, 3.0 mL of the supernatant were passed through a 70-μm-pore size nylon mesh filter. The cells were washed once with DMEM containing 0.5 mg/mL DNase I (Roche). The cells were then suspended with 2 mL of DMEM containing 10% fetal calf serum, 2 mM L-glutamine and 25 mM KCl (Nagata & Nakatsuji, 1990). During incubation at 37 °C for 24 h in a humidified atmosphere with 5% CO_2, the granule cells aggregated. The reaggregates were plated at a density of 15–30 clusters/20 mm^2 on glass coverslips (CELLocate, Eppendorf, Hamburg, Germany) coated with poly L-lysine (100 μg/mL) and laminin (20 μg/mL). The cells were incubated at 37 °C in 5% CO_2 for 1 h to allow the cell reaggregates to adhere to the coated glass, and then 2 mL of DMEM containing 10% fetal calf serum, 2 mM L-glutamine and 25 mM KCl were further added. After the cells were incubated for 15–20 h in 5% CO_2, the microscopic measurements of the migration were initiated.

Immunostaining

Reaggregate cell clusters were cultured on poly L-lysine-coated and laminin-coated glass bottom culture dishes (Mat Tek Corporation, Ashland, MA, USA). The cells were fixed for 20 min with 4% paraformaldehyde, blocked and permeabilized for 20 min with 10% goat serum and 0.1% Triton X-100 in phosphate-buffered saline. The primary antibody, i.e. an anticlass III β-tubulin (TUJ-1; 1 : 1000, monoclonal, Babco, Berkley, CA) or an antiglial fibrillary acidic protein (GFAP) antibody (1 : 1, polyclonal, DAKO, Carpinteria, CA, USA), was applied to the cells for 1 h. The cells were rinsed with phosphate-buffered saline, and re-permeabilized for 20 min with 10% goat serum and 0.1% Triton X-100 in phosphate-buffered saline. The appropriate secondary antibodies (fluorescein- or Texas Red-conjugated, 1 : 100) were then applied for 1 h, followed by a single rinse with phosphate-buffered saline. The cells were observed for fluorescence with an LSM 510 Laser Scanning Microscope System (Carl Zeiss, Oberkochen, Germany).

Western blotting

Cerebellar granule cells were prepared from P3 mice. The cells were lysed by the addition of a 2 × SDS-PAGE sample buffer (50 mM Tris-HCl pH 6.5, 10% glycerol, 2% SDS, 0.5% bromophenol blue and 2% 2-mercaptoethanol) and DNA was sheared by ten passes through a 27-gauge needle. Each lysate was subjected to SDS-PAGE, and the separated proteins were transferred to a nitrocellulose filter (Hybond ECL, Amersham-Pharmacia Biotech, Arlington Heights, IL). The filter was blocked with nonfat milk (BlockAce; Dainippon Medical, Osaka, Japan) at 4 °C overnight and incubated with an anti-LIS1 monoclonal antibody (a gift from Drs J. Aoki and H. Arai, University of Tokyo, Tokyo, Japan) or a rabbit anti-NUDEL polyclonal antibody (Sasaki *et al.*, 2000) in Tris-buffered saline (pH 8.0) containing 0.05% Tween 20 (TBS-T), and then treated with anti-mouse IgG conjugated to horseradish peroxidase (Cappel, Aurora, OH, USA) or anti-rabbit IgG conjugated to horseradish peroxidase (Amersham-Pharmacia Biotech.). The proteins bound to the antibodies were visualized using an enhanced chemiluminescence kit (ECL, Amersham-Pharmacia Biotech).

Time-lapse observation of granule cell migration in vitro

Fifteen to twenty hours after plating, the dishes were transferred into the chamber of a microincubator (Sankei, Tokyo, Japan) attached to the stage of a phase-contrast microscope (Nikon, Tokyo, Japan). The chamber temperature was kept at 37 °C using a temperature controller (Kokensha Engineering, Tokyo, Japan), and the cells were provided with a constant gas flow (95% air, 5% CO_2). Five minutes after the dish was transferred into the chamber, the observation was started. Images were projected to a CCD camera (Nikon) and recorded onto a laser videodisc recorder, LVR-3000AV (SONY, Tokyo, Japan) every 10 min for 60 min. These data were analyzed on Macintosh computers using NIH Image software (version 1.61). Thirty peripheral cells on the

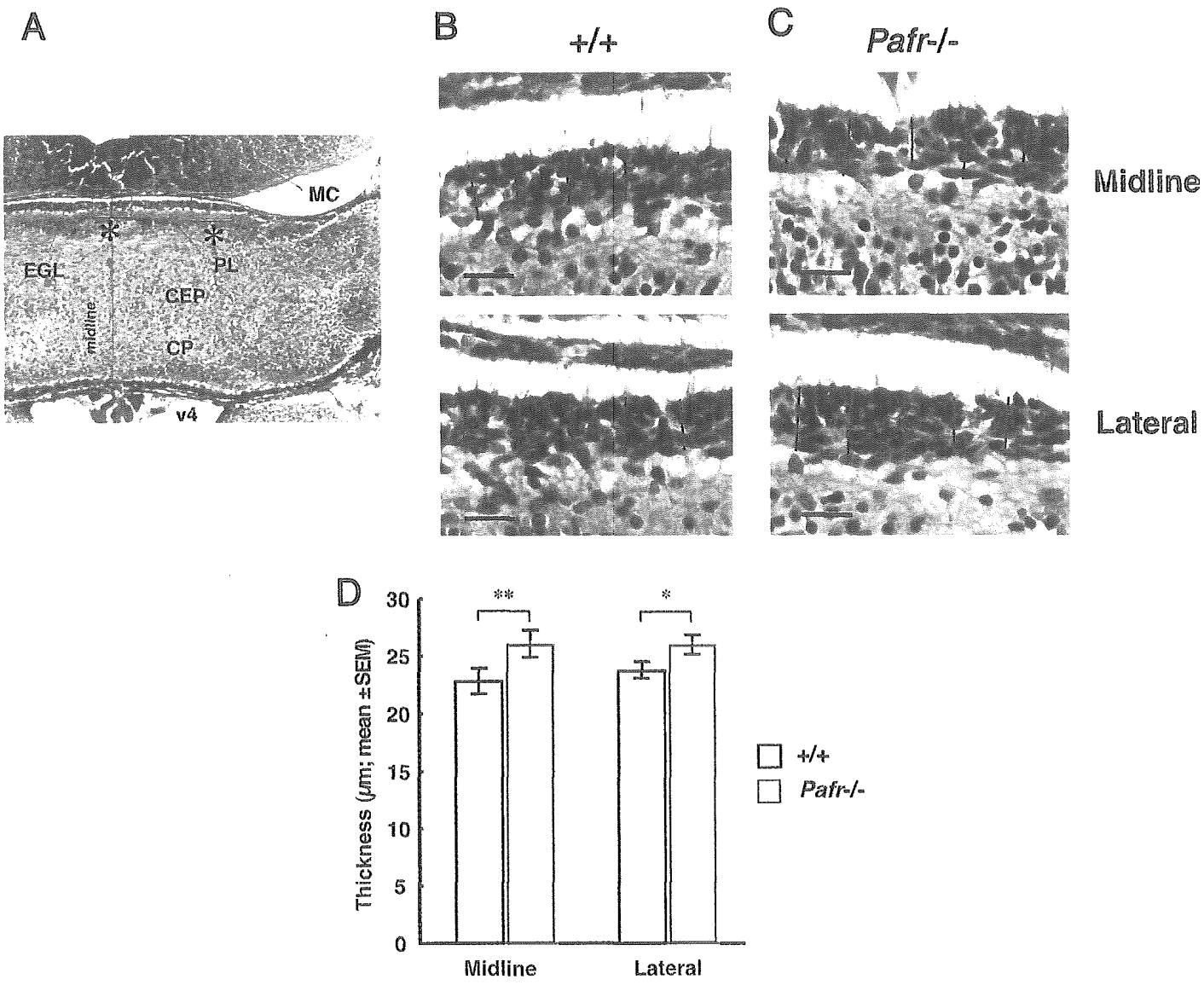

FIG. 1. Abnormalities in the cerebellum of embryonic *Pafr−/−* mice. (A–C) Cross-sections of E17.5 cerebella were stained with haematoxylin and eosin. Coronal sections were made and two parts of the EGL were set for the measurements as indicated in A, one on the midline and the other at 300 μm lateral to the midline. The thickness of the layer was measured at five points 20 μm apart from each other in the 80-μm-long segments as indicated in B (wild-type, +/+) and C (*Pafr−/−*). (D) The mean values of the thickness were evaluated. The EGL of the cerebellum of *Pafr−/−* mice is significantly thicker than that of the wild-type mice both at the midline (left) and at 300 μm lateral to the midline (right). $^{**}P < 0.005$, $^{*}P < 0.05$ for comparison between littermates (paired *t*-test, $n = 8$). Scale bars, 25 μm in B and C. (CEP, cerebellar primordium; EGL, external granular layer; PL, Purkinje cell layer; CP, choroid plexus; MC, mesencephalon; v4, the fourth ventricle.)

extended neurites from the reaggregates were chosen randomly in one culture dish. The distances each cell travelled during each 10-min interval were integrated. The experiment was repeated to determine the mean migration distance of all cells.

Statistics

Statistical analysis was performed using StatView (version 5.0) software (SAS Institute, Cary, NC, USA). A *P*-value less than 0.05 was taken to be statistically significant.

Chemicals

WEB 2086 was a generous gift from Boehringer–Ingelheim (Ingelheim Germany), which was dissolved in DMEM by bath sonication at a stock concentration of 5 mM. Methylcarbamyl platelet-activating factor (mc-PAF, 1-*O*-hexadecyl-2-*O*-(methylcarbamyl)-*sn*-glycero-3-phosphocholine) was obtained from Cayman Chemical (Ann Arbor, MI, USA). Laminin, natural preparation of mouse laminin isolated from Engelbreth–Holm–Swarm (EHS) sarcoma, was obtained from Invitrogen. All other reagents, unless otherwise stated, were from Wako (Osaka, Japan) or Sigma (St. Louis, MD, USA).

Results

Morphological abnormalities in the cerebellum of embryonic Pafr−/− mice

Histological examinations revealed no obvious gross anomaly in the brains of 1-day-old, 3-, 5-, or 8-week-old *Pafr−/−* mice (data not shown). In embryonic *Pafr−/−* mice, however, we found minute but significant abnormalities in the cerebellum. The EGL of the cerebellum of *Pafr−/−* mice at embryonic day 17.5 (E17.5) was significantly thicker than that of the wild-type mice (Fig. 1B and C). A similar trend was seen in the E14.5 cerebellum, although the difference was not

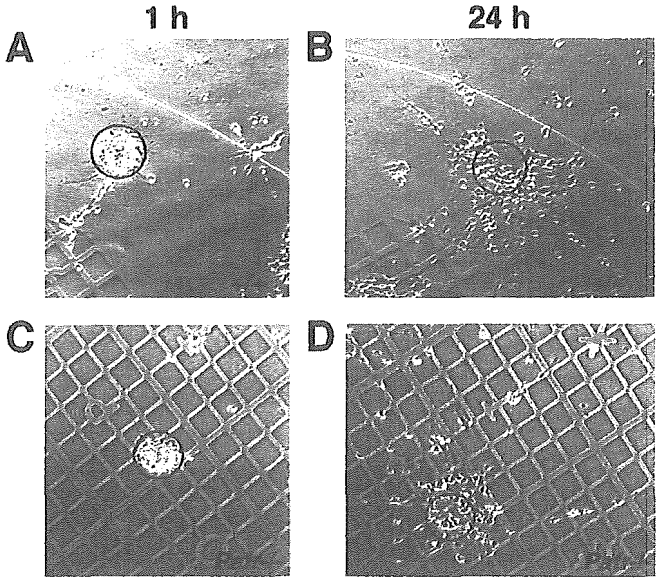

FIG. 2. Reaggregate cultures of cerebellar granule cells. Cerebellar granule cells from wild-type (+/+) (A, B) and *Pafr*−/− (C, D) mice at P2 were prepared and incubated for 24 h to form reaggregate cell clusters. The clusters were plated on glass cover slips coated with poly L-lysine and laminin. A and C show examples of clusters 1 h after plating and B and D show the same clusters 24 h after plating. The circles show the original locations of the plated clusters. Grid: 55-μm square size.

statistically significant ($P = 0.0781$, paired t-test) (data not shown). No obvious morphological differences were seen in the cerebral cortex at E17.5 (data not shown).

Abnormalities in in vitro *migration of Pafr−/− neurons*

As *Lis1*+/− mice have been reported to have defects in neuronal migration and layering *in vivo*, and also in cerebellar granule cell migration *in vitro*, we examined the unidirectional *in vitro* migration of the granule cells. To compare the migration rate of wild-type neurons and *Pafr*−/− neurons, cerebellar cell reaggregates on a laminin substrate were used (Adachi *et al.*, 1997; Bix & Clark, 1998; Hirotsune *et al.*, 1998). Figure 2 depicts the *in vitro* spontaneous cell migration of cerebellar granule neurons derived from wild-type and *Pafr*−/− mice 24 h after plating. The cerebellar granule cells can easily be identified by their bipolar, spindle-shaped morphology with neurites. These neurites were positive for TUJ-1, a neuronal class III β-tubulin-specific marker (data not shown). Neuronal migration along preextended neurites was observed in each reaggregate by time-lapse video microscopy. In this primary culture system, there were a few cells that were positive for GFAP, a glial cell marker. The glial contents were similar between wild-type and *Pafr*−/−, and the ratios of the GFAP-positive cell number to the total cell number were 3.28 ± 0.65% and 3.30 ± 0.46%, respectively (mean ± SEM, $n = 3$). The total cell numbers of GFAP-positive cells were 109 out of 3121 and 127 out of 3854, respectively.

The migration of *Pafr*−/− cells was significantly slower than that of wild-type cells (Fig. 3A, wild-type 21.1 ± 1.02 μm; *Pafr*−/− 14.4 ± 0.9 μm, $P < 0.001$, ANOVA with Scheffe's *posthoc* test). When granule cells were treated with a PAF receptor antagonist, WEB 2086, the migration distance of wild-type cells was reduced to the same level as *Pafr*−/− cells (Fig. 3A, 21.1 ± 1.0 μm at 0 μM; 15.4 ± 1.0 at 150 μM, $P = 0.002$, ANOVA with Scheffe's *posthoc* test). On the other hand, WEB 2086 had no apparent effects on *Pafr*−/− cells (Fig. 3A). The distribution of the migration distance in 60 min is shown in Fig. 3B and

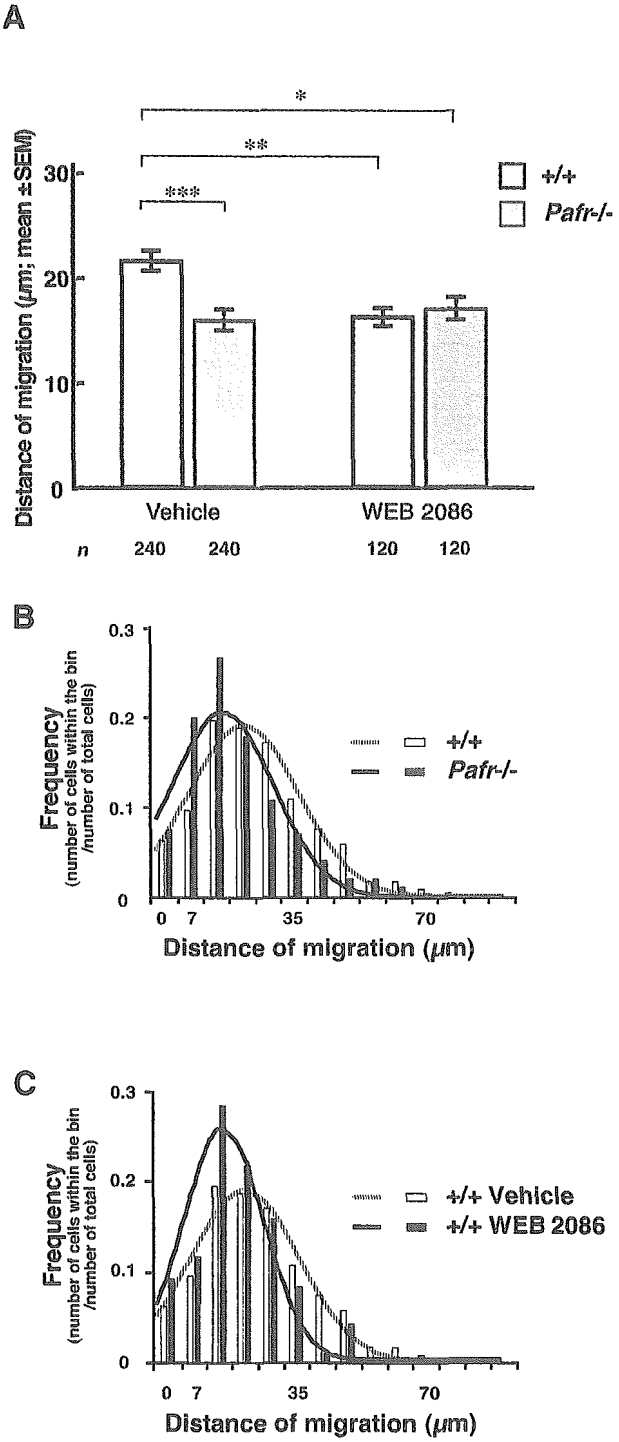

FIG. 3. Effect of PAF receptor on granule cell migration *in vitro*. (A) Reaggregate cell clusters from wild-type (+/+) mice or *Pafr*−/− mice were treated with vehicle or 150 μM WEB 2086 for 60 min before observation. Cell migration was quantified as described under Materials and methods by time-lapse observation for 60 min. The data were obtained from four mice of each genotype, and represent the mean ± SEM. The number (n) of cells observed is indicated. $^{***}P < 0.001$, $^{**}P < 0.005$, $^{*}P < 0.05$ vs. vehicle-treated wild-type as determined by analysis of variance (ANOVA) with Scheffe's test. (B and C) The x-axis is divided into 7 μm-bins, and the y-axis represents the ratio of the number of cells migrates within the bin to the total cell number. The smooth lines correspond to fit to a Gaussian function. B shows the distribution of the migration distance of wild-type and *Pafr*−/− neurons. C shows the distribution of the migration distance of vehicle-treated wild-type and WEB 2086-treated wild-type neurons.

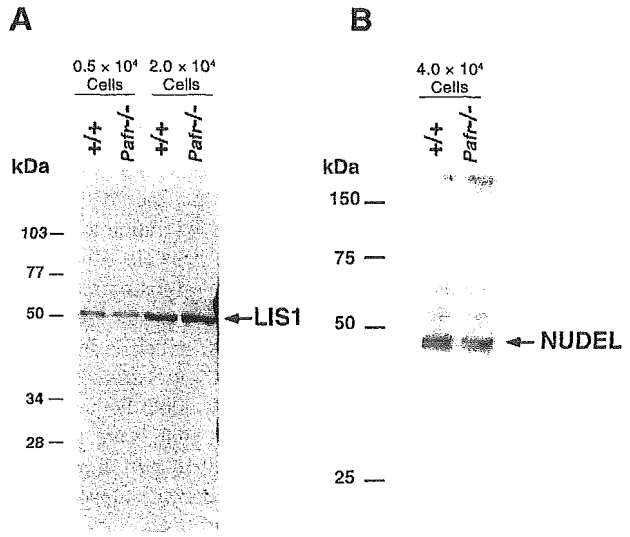

FIG. 4. Expression of LIS1 and NUDEL in wild-type and *Pafr*−/− cerebellar granule cells. Western blot analyses of LIS1 and NUDEL in wild-type (+/+) and *Pafr*−/− cerebellar granule cells at P3 were performed using an anti-LIS1 antibody (A) and an anti-NUDEL antibody (B). Whole cell lysates from the indicated numbers of cells were loaded in each lane.

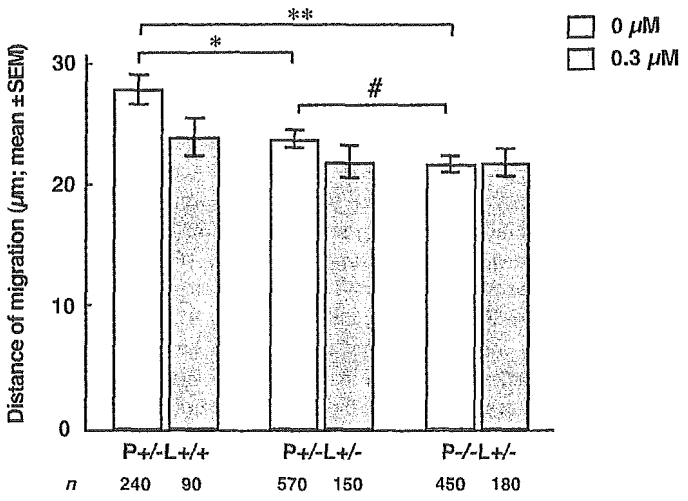

FIG. 5. Effect of LIS1 on the granule cell migration of *Pafr*−/− cells *in vitro*. Reaggregate cell clusters from *Pafr*+/−*Lis1*+/+ (P+/−L+/+), *Pafr*+/−*Lis1*+/− (P+/−L+/−) and *Pafr*−/−*Lis1*+/− (P−/−L+/−) mice were treated with vehicle or 0.3 μM mc-PAF for 60 min before observation. The data represent the mean ± SEM and were obtained from three P+/−L+/+ mice, six P+/−L+/− mice and five P−/−L+/− mice. The number (*n*) of cells observed is indicated. $^{**}P < 0.005$ and $^{*}P < 0.05$ vs. vehicle-treated P+/−L+/+and $\#P < 0.005$ vs. vehicle-treated P+/−L+/−, as determined by ANOVA with Fisher's test.

C. Althought not specific, the overall population of *Pafr*−/− cells shifted to the left compared to the wild-type cells (Fig. 3B). After treatment with WEB 2086, the distribution of the migration distance of wild-type cells became similar to that of *Pafr*−/− cells (Fig. 3C). These results suggest that intrinsic PAF exerts a stimulatory effect on the neuronal migration through a PAF receptor.

Expression of LIS1 and NUDEL in cerebellar granule cells

As reduction of LIS1 protein leads to abnormal neuronal migration (Hirotsune *et al.*, 1998; Cahana *et al.*, 2001), we examined whether or not the LIS1 expression level is decreased in *Pafr*−/− mice. Immunoblot analysis of whole cell lysates from neonatal cerebellar cells with an anti-LIS1 monoclonal antibody demonstrated that the LIS1 expression level was not different between wild-type and *Pafr*−/− cerebellar cells (Fig. 4A). NUDEL is one of the LIS1 interacting proteins previously reported by several groups and is thought to play a role in neuronal migration by interacting with LIS1 (Feng *et al.*, 2000; Kitagawa *et al.*, 2000; Niethammer *et al.*, 2000; Sasaki *et al.*, 2000). As in the case of LIS1, no significant difference in NUDEL expression was seen between wild-type and *Pafr*−/− mice (Fig. 4B).

Effect of reduction of LIS1 expression on neuronal migration in Pafr−/− cells

We generated double mutant mice: *Pafr* heterozygous- or homozygous-deficient and *Lis1* heterozygous-deficient (*Pafr*+/−*Lis1*+/− or *Pafr*−/−*Lis1*+/−). Both *Pafr*+/−*Lis1*+/− and *Pafr*−/−*Lis1*+/− mice grew with no apparent abnormalities except for a reduction of fertilization (S. M. Tokuoka & S. Ishii, unpublished observation). The brain disorganization of these mice was similar to the *Lis1*+/− phenotype (data not shown). As *Pafr*+/− mice have no defects, including the response to PAF, *Pafr*+/−*Lis1*+/+neurons derived from littermates were used as a substitute for wild-type controls. The migration of *Pafr*+/−*Lis1*+/− (the middle white column in Fig. 5) neurons *in vitro* was significantly reduced as compared to *Pafr*+/−*Lis1*+/+neurons (the left white column), consistent with a previous report (Hirotsune *et al.*, 1998). Interestingly, further reduction of migration was observed in *Pafr*−/−*Lis1*+/− neurons (the right white column in Fig. 5), or WEB 2086-treated *Pafr*+/−*Lis1*+/− neurons (control, 23.2 ± 2.2 μm, $n = 180$; WEB 2086, 19.4 ± 1.4 μm, $n = 150$, $P < 0.05$). This reduction caused by the PAF receptor deficiency, either genetically or pharmacologically, suggests that PAF receptor and LIS1 may act synergistically in neuronal cell migration.

Effect of PAF on the migration of Pafr−/− cells

Next, we examined the effect of PAF receptor activation by an exogenous agonist. As an agonist for PAF receptor, we used mc-PAF, because this PAF analogue is resistant to degradation by PAF acetylhydrolases present in brain and plasma (Hattori *et al.*, 1993;

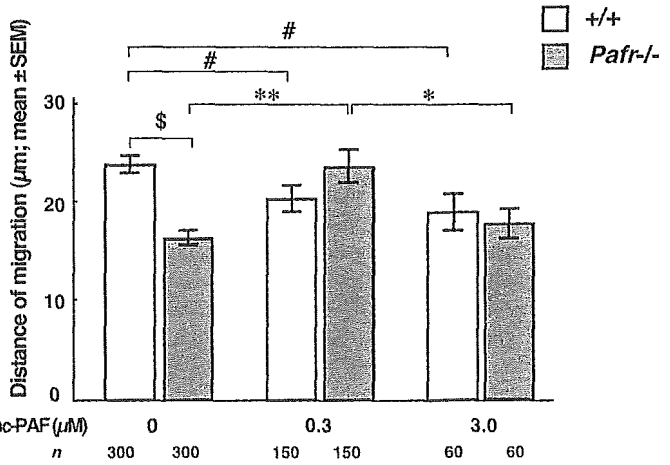

FIG. 6. Effect of mc-PAF on the granule cell migration *in vitro*. Reaggregate cell clusters from wild-type (+/+) mice or *Pafr*−/− mice were treated with vehicle or the indicated concentrations of mc-PAF for 60 min before observation. The data represent the mean ± SEM and *n* indicates the number of cells observed. The cells were obtained from five mice of each genotype. $\$P < 0.001$ vs. vehicle-treated wild-type cells as determined by unpaired *t*-test. $^{**}P < 0.001$ and $^{*}P < 0.05$ vs. 0.3 μM mc-PAF-treated *Pafr*−/− cells by ANOVA with Scheffe's test. $\#P < 0.05$ vs. vehicle-treated wild-type cells by ANOVA with Fisher's test.

Tjoelker *et al.*, 1995). Mc-PAF was reported to have a K_d value five-fold higher than PAF in neutrophils, and the agonistic effect of mc-PAF is weaker than that of PAF (O'Flaherty *et al.*, 1987). In wild-type cells, as reported previously (Adachi *et al.*, 1997; Bix & Clark, 1998), mc-PAF inhibited cell migration in a dose-dependent manner (Fig. 6). Unexpectedly, the effect of mc-PAF on *Pafr−/−* neurons was also observed, in that 0.3 μM mc-PAF significantly promoted rather than inhibited the cell migration. A higher concentration of mc-PAF (3 μM), however, did not show such a stimulatory effect (Fig. 6).

The migration of *Pafr+/−Lis1+/−* neurons was significantly inhibited by 0.3 μM mc-PAF (the grey columns in Fig. 5). The migration of *Pafr−/−Lis1+/−* neurons was not affected by 0.3 μM mc-PAF, which markedly contrasts with the data that the migration of *Pafr−/−Lis1+/+* neurons was accelerated by the same concentration of mc-PAF (Fig. 6). These results suggest that the responsiveness to mc-PAF of *Pafr−/−* neurons is dependent on LIS1 protein.

Discussion

The migration of neurons is a critical process in brain development. It requires three main steps: (i) extension of the leading edge, (ii) movement of the nucleus into the leading process, called nucleokinesis, and (iii) retraction of the trailing process. Cerebellar granule cells are often used for the study of neuronal migration because of the clearly distinguishable shape, the location in the cerebellar cortex, dynamic migration, and well-established culture systems (Nagata & Nakatsuji, 1990; Asou *et al.*, 1992; Komuro & Rakic, 1995). By time-lapse microscopic observation of cerebellar granule cell reaggregates, we showed reduction of the migration of *Pafr−/−* neurons and also of PAF antagonist-treated wild-type neurons (Fig. 3). These results suggest that intrinsic PAF stimulates neuronal migration through the PAF receptor. The production of PAF in these cells was reported previously (Yue *et al.*, 1990).

Little is known about the molecular basis underlying neuronal migration. Previous studies have suggested that granule cell migration could be modulated by intrinsic Ca^{2+} fluctuations or Ca^{2+} elevation by external stimuli, such as somatostatin or stromal cell-derived factor 1α (SDF-1α) (Komuro & Rakic, 1996; Klein *et al.*, 2001; Yacubova & Komuro, 2002). PAF receptor stimulation evokes intracellular Ca^{2+} elevation in various cells including neurons (Bito *et al.*, 1992; Ishii & Shimizu, 2000). Another intracellular signalling pathway of the PAF receptor may account for the effect of PAF on the neuronal migration, as PAF was reported to activate glycogen synthase kinase 3β (GSK-3β) (Tong *et al.*, 2001) which is involved in microtubule rearrangement and the phosphorylation of microtubule-associated proteins (Goold *et al.*, 1999). In addition to triggering intracellular signallings, PAF receptor may bring PAF into granule cells. Many G-protein-coupled receptors, including PAF receptor, internalize into cells with their agonists in response to ligand stimulation (Le Gouill *et al.*, 1997; Ishii *et al.*, 1998a; Ohshima *et al.*, 2002). Thus, it is possible that PAF receptor acts as a transporter for PAF, delivering it to putative intracellular target molecules related to neuronal migration (see below).

The migration of *Pafr−/−Lis1+/−* cells was significantly slower than that of *Pafr+/−Lis1+/−* cells (the right white column vs. the middle white column in Fig. 5). As shown in Fig. 3A (left columns), we obtained similar results from LIS1-intact cells, i.e. *Pafr+/+Lis1+/+* and *Pafr−/−Lis1+/+*. However, PAF receptor deficiency seems to impair the migration ability less in *Lis1+/−* (8.6% reduction) than in *Lis1+/+* (26.1% reduction). These data imply that LIS1 is involved in the stimulation of neuronal migration by PAF receptor.

We also found that exogenous mc-PAF inhibits neuronal migration in wild-type cells (Fig. 6), as reported previously (Adachi *et al.*, 1997; Bix & Clark, 1998). This looks contradictory to the pharmacological and genetic results that intrinsic PAF exerts a stimulatory effect on the neuronal migration through a PAF receptor (Fig. 3). The inhibition by 0.3 μM mc-PAF and 150 μM WEB 2086 may not be due to nonspecific neurotoxicity of the compounds because 0.3 μM mc-PAF stimulated and 150 μM WEB 2086 did not affect the migration of *Pafr−/−* neurons (Figs 6 and 3A, respectively). One possible explanation is that the dose-dependent effect of PAF on the migration may be bell-shaped and that the concentration of intrinsic PAF in the culture may be optimal for the migration of wild-type cells, which is inhibited by WEB 2086. The bell-shaped dose-dependency was also observed in chemotaxis in response to PAF (Aihara *et al.*, 2000; Fukunaga *et al.*, 2001). Chemotaxis and neuronal migration may have a common regulatory mechanism that results in the bell-shaped dose–response curve. However, it should be noted that high concentrations of mc-PAF may inhibit neuronal migration by its neurotoxicity, as suggested previously (Bennett *et al.*, 1998; Tong *et al.*, 2001; Brewer *et al.*, 2002).

In this study, we showed that 0.3 μM mc-PAF promoted neuronal migration of *Pafr−/−* granule cells, raising the possibility of a receptor-independent pathway(s) for PAF action (Fig. 6). This includes the presence of the putative 'second' PAF receptor and uptake of PAF by the flip-flop mechanism (Menon, 1995).

As the accelerating effect of mc-PAF was undetectable in *Pafr−/−Lis1+/−* cells (Fig. 5), LIS1 protein appears to be involved in the receptor–independent PAF action. LIS1 is a subunit of a brain PAF acetylhydrolase, forming a heterotrimeric complex with two catalytic subunits, 29 kDa α1 subunit and 30 kDa α2 subunit. Furthermore, LIS1 interacts with microtubules, cytoplasmic dynein, dynactin, mNudE, and NUDEL, regulating the microtubule cytoskeleton (Wynshaw-Boris & Gambello, 2001). Thus, intracellular PAF might affect the interactions of LIS1 with these molecules, especially with PAF acetylhydrolase α subunits. Indeed, a previous report demonstrated that all of the examined human LIS1 mutations abolished or reduced the capacity of LIS1 to interact with the α subunits in the yeast two-hybrid system and GST pulldown experiments, suggesting that the formation of the brain PAF acetylhydrolase complex seems to be important for the neuronal migration (Sweeney *et al.*, 2000). A compositional change in the LIS1 complex may regulate LIS1 functions in microtubule reorganization and neuronal migration.

We found abnormalities of the EGL of *Pafr−/−* cerebellum at E17.5 (Fig. 1C). Cerebellar granule cell progenitors are produced in the rhombic lip, a specialized germinative epithelium that arises at the interface between the neural tube and the roofplate of the fourth ventricle. Then at E13–14, the cells migrate over the cerebellar primordium to form a secondary proliferative zone, EGL. During early postnatal development, granule cell precursors in the outer zone of the EGL proliferate, differentiate and migrate radially to the internal granular cell layer, IGL (Goldowitz & Hamre, 1998). It should be noted that postmitotic cerebellar granule cells start to migrate parallel to the cerebellar surface (tangentially) before the onset of their radial migration (Ryder & Cepko, 1994; Komuro *et al.*, 2001). The cerebellar abnormality in *Pafr−/−* mice therefore may be caused by a defect of the tangential neuronal migration within the EGL as observed in *Pax6* mutants (Engelkamp *et al.*, 1999; Yamasaki *et al.*, 2001), although we cannot rule out the possibility that the defect in the E17.5 cerebellum is caused by abnormal proliferation in the EGL. Consistently, we demonstrated that PAF receptor affected neuronal migration *in vitro* using granule cells derived from mice at P2–P4. At this stage, cerebellum contains a few radially migrating neurons, and many immature granule neurons, which exist in the EGL, some of which are migrating

tangentially within the EGL. In this culture system, we observed the migration of bipolar granule neurons along these neurites. This mode of migration in culture, as suggested previously (Nagata & Nakatsuji, 1990), might be relevant to the tangential migration (Yamasaki *et al.*, 2001). Thus, our observation, both *in vivo* and *in vitro*, may reflect the abnormality of the tangential migration of granule cells within the EGL. No apparent histological abnormalities were seen in the adult brain, and the thickness of the EGL at P5 was indistinguishable between wild-type and *Pafr−/−* mice (data not shown). These findings suggest either minor roles of PAF and its receptor in neuronal development, or redundancy of the second type of the PAF receptor.

Nevertheless, we showed significant abnormalities in neuronal migration both *in vivo* and *in vitro* for the first time using *Pafr−/−* and *Lis1+/−* mice. Our results suggest that cerebellar granule cell migration is regulated by PAF through receptor-dependent and receptor-independent pathways and that LIS1 is a pivotal molecule that links PAF action and neuronal cell migration both *in vivo* and *in vitro*.

Acknowledgements

S.M.T. was a recipient of the Fellowship for Young Scientists from Japan Society for the Promotion of Science. This work was supported in part by a Grant-in-Aid from the Ministry of Education, Science, Culture, Sports and Technology of Japan, Grants-in-Aid for Comprehensive Research on Ageing and Health, and for Research on Allergic Disease and Immunology from the Ministry of Health, Labour and Welfare, Japan, and grants from the Yamanouchi Foundation for Research on Metabolic Disorders, from the Kanae Foundation for Life and Socio-medical Science, and from the Uehara Memorial Foundation. (S.I). We are grateful to Drs T. Adachi and H. Aso (Tokyo Metropolitan Institute of Gerontology) for instructing granule cell reaggregate cultures, and Drs J. Aoki and H. Arai (The University of Tokyo) for providing an anti-LIS1 monoclonal antibody. We also thank Drs J. Aruga, M. Ogawa, and T. Miyata (RIKEN, Saitama, Japan), Dr I. Nagata (Tokyo Metropolitan Institute for Neuroscience), and Drs H. Bito and S. Nonaka (The University of Tokyo) for valuable suggestions.

Abbreviations

DMEM, Dulbecco's modified Eagle's medium; EGL, external granular layer; PAF, platelet-activating factor, 1-*O*-alkyl-sn-glycero-3-phosphorylcholine; PAFR, platelet-activating factor receptor; *Pafr−/−*, PAF receptor-deficient; mc-PAF, methylcarbamyl platelet-activating factor.

References

Adachi, T., Aoki, J., Manya, H., Asou, H., Arai, H. & Inoue, K. (1997) PAF analogues capable of inhibiting PAF acetylhydrolase activity suppress migration of isolated rat cerebellar granule cells. *Neurosci. Lett.*, **235**, 133–136.

Aihara, M., Ishii, S., Kume, K. & Shimizu, T. (2000) Interaction between neurone and microglia mediated by platelet-activating factor. *Genes Cells*, **5**, 397–406.

Asou, H., Miura, M., Kobayashi, M., Uyemura, K. & Itoh, K. (1992) Cell adhesion molecule L1 guides cell migration in primary reaggregation cultures of mouse cerebellar cells. *Neurosci. Lett.*, **144**, 221–224.

Baker, R.R. (1995) Enzymes of platelet activating factor synthesis in brain. *Neurochem. Res.*, **20**, 1345–1351.

Bennett, S.A., Chen, J., Pappas, B.A., Roberts, D.C. & Tenniswood, M. (1998) Platelet activating factor receptor expression is associated with neuronal apoptosis in an *in vivo* model of excitotoxicity. *Cell Death Differ.*, **5**, 867–875.

Bito, H., Nakamura, M., Honda, Z., Izumi, T., Iwatsubo, T., Seyama, Y., Ogura, A., Kudo, Y. & Shimizu, T. (1992) Platelet-activating factor (PAF) receptor in rat brain: PAF mobilizes intracellular Ca^{2+} in hippocampal neurons. *Neuron*, **9**, 285–294.

Bix, G.J. & Clark, G.D. (1998) Platelet-activating factor receptor stimulation disrupts neuronal migration *in vitro*. *J. Neurosci.*, **18**, 307–318.

Brewer, C., Bonin, F., Bullock, P., Nault, M.C., Morin, J., Imbeault, S., Shen, T.Y., Franks, D.J. & Bennett, S.A. (2002) Platelet activating factor-induced apoptosis is inhibited by ectopic expression of the platelet activating factor G-protein coupled receptor. *J. Neurochem.*, **82**, 1502–1511.

Cahana, A., Escamez, T., Nowakowski, R.S., Hayes, N.L., Giacobini, M., von Holst, A., Shmueli, O., Sapir, T., McConnell, S.K., Wurst, W., Martinez, S. & Reiner, O. (2001) Targeted mutagenesis of Lis1 disrupts cortical development and LIS1 homodimerization. *Proc. Natl Acad. Sci. USA*, **98**, 6429–6434.

Chen, C., Magee, J.C., Marcheselli, V., Hardy, M. & Bazan, N.G. (2001) Attenuated LTP in hippocampal dentate gyrus neurons of mice deficient in the PAF receptor. *J. Neurophysiol.*, **85**, 384–390.

Clark, G.D., Happel, L.T., Zorumski, C.F. & Bazan, N.G. (1992) Enhancement of hippocampal excitatory synaptic transmission by platelet-activating factor. *Neuron*, **9**, 1211–1216.

DeCoster, M.A., Mukherjee, P.K., Davis, R.J. & Bazan, N.G. (1998) Platelet-activating factor is a downstream messenger of kainate-induced activation of mitogen-activated protein kinases in primary hippocampal neurons. *J. Neurosci. Res.*, **53**, 297–303.

Engelkamp, D., Rashbass, P., Seawright, A. & van Heyningen, V. (1999) Role of Pax6 in development of the cerebellar system. *Development*, **126**, 3585–3596.

Feng, Y., Olson, E.C., Stukenberg, P.T., Flanagan, L.A., Kirschner, M.W. & Walsh, C.A. (2000) LIS1 regulates CNS lamination by interacting with mNudE, a central component of the centrosome. *Neuron*, **28**, 665–679.

Fukunaga, K., Ishii, S., Asano, K., Yokomizo, T., Shiomi, T., Shimizu, T. & Yamaguchi, K. (2001) Single nucleotide polymorphism of human platelet-activating factor receptor impairs G-protein activation. *J. Biol. Chem.*, **276**, 43025–43030.

Gelbard, H.A., Nottet, H.S., Swindells, S., Jett, M., Dzenko, K.A., Genis, P., White, R., Wang, L., Choi, Y.B., Zhang, D., Lipton, S.A., Tourtellotte, W.W., Epstein, L.G. & Gendelman, H.E. (1994) Platelet-activating factor: a candidate human immunodeficiency virus type 1-induced neurotoxin. *J. Virol.*, **68**, 4628–4635.

Goldowitz, D. & Hamre, K. (1998) The cells and molecules that make a cerebellum. *Trends Neurosci.*, **21**, 375–382.

Goold, R.G., Owen, R. & Gordon-Weeks, P.R. (1999) Glycogen synthase kinase 3β phosphorylation of microtubule-associated protein 1B regulates the stability of microtubules in growth cones. *J. Cell Sci.*, **112**, 3373–3384.

Grassi, S., Francescangeli, E., Goracci, G. & Pettorossi, V.E. (1998) Role of platelet-activating factor in long-term potentiation of the rat medial vestibular nuclei. *J. Neurophysiol.*, **79**, 3266–3271.

Hattori, M., Adachi, H., Aoki, J., Tsujimoto, M., Arai, H. & Inoue, K. (1995) Cloning and expression of a cDNA encoding the β-subunit (30-kDa subunit) of bovine brain platelet-activating factor acetylhydrolase. *J. Biol. Chem.*, **270**, 31345–31352.

Hattori, M., Adachi, H., Tsujimoto, M., Arai, H. & Inoue, K. (1994a) The catalytic subunit of bovine brain platelet-activating factor acetylhydrolase is a novel type of serine esterase. *J. Biol. Chem.*, **269**, 23150–23155.

Hattori, M., Adachi, H., Tsujimoto, M., Arai, H. & Inoue, K. (1994b) Miller-Dieker lissencephaly gene encodes a subunit of brain platelet-activating factor acetylhydrolase. *Nature*, **370**, 216–218.

Hattori, M., Arai, H. & Inoue, K. (1993) Purification and characterization of bovine brain platelet-activating factor acetylhydrolase. *J. Biol. Chem.*, **268**, 18748–18753.

Henneberry, A.L., Wistow, G. & McMaster, C.R. (2000) Cloning, genomic organization, and characterization of a human cholinephosphotransferase. *J. Biol. Chem.*, **275**, 29808–29815.

Hirotsune, S., Fleck, M.W., Gambello, M.J., Bix, G.J., Chen, A., Clark, G.D., Ledbetter, D.H., McBain, C.J. & Wynshaw-Boris, A. (1998) Graded reduction of Pafah1b1 (Lis1) activity results in neuronal migration defects and early embryonic lethality. *Nature Genet.*, **19**, 333–339.

Honda, Z., Ishii, S. & Shimizu, T. (2002) Platelet-activating factor receptor. *J. Biochem. (Tokyo)*, **131**, 773–779.

Honda, Z., Nakamura, M., Miki, I., Minami, M., Watanabe, T., Seyama, Y., Okado, H., Toh, H., Ito, K., Miyamoto, T. & Shimizu, T. (1991) Cloning by functional expression of platelet-activating factor receptor from guinea-pig lung. *Nature*, **349**, 342–346.

Ishii, S., Matsuda, Y., Nakamura, M., Waga, I., Kume, K., Izumi, T. & Shimizu, T. (1996) A murine platelet-activating factor receptor gene: cloning, chromosomal localization and up-regulation of expression by lipopolysaccharide in peritoneal resident macrophages. *Biochem. J.*, **314**, 671–678.

Ishii, I., Saito, E., Izumi, T., Ui, M. & Shimizu, T. (1998a) Agonist-induced sequestration, recycling, and resensitization of platelet-activating factor receptor. Role of cytoplasmic tail phosphorylation in each process. *J. Biol. Chem.*, **273**, 9878–9885.

Ishii, S., Kuwaki, T., Nagase, T., Maki, K., Tashiro, F., Sunaga, S., Cao, W.H., Kume, K., Fukuchi, Y., Ikuta, K., Miyazaki, J., Kumada, M. & Shimizu, T. (1998b) Impaired anaphylactic responses with intact sensitivity to endotoxin in mice lacking a platelet-activating factor receptor. *J. Exp. Med.*, **187**, 1779–1788.

Ishii, S. & Shimizu, T. (2000) Platelet-activating factor (PAF) receptor and genetically engineered PAF receptor mutant mice. *Prog. Lipid Res.*, **39**, 41–82.

Kanowski, S., Herrmann, W.M., Stephan, K., Wierich, W. & Horr, R. (1996) Proof of efficacy of the ginkgo biloba special extract EGb 761 in outpatients suffering from mild to moderate primary degenerative dementia of the Alzheimer type or multi-infarct dementia. *Pharmacopsychiatry*, **29**, 47–56.

Kato, K., Clark, G.D., Bazan, N.G. & Zorumski, C.F. (1994) Platelet-activating factor as a potential retrograde messenger in CA1 hippocampal long-term potentiation. *Nature*, **367**, 175–179.

Kitagawa, M., Umezu, M., Aoki, J., Koizumi, H., Arai, H. & Inoue, K. (2000) Direct association of LIS1, the lissencephaly gene product, with a mammalian homologue of a fungal nuclear distribution protein, rNUDE. *FEBS Lett.*, **479**, 57–62.

Klein, R.S., Rubin, J.B., Gibson, H.D., DeHaan, E.N., Alvarez-Hernandez, X., Segal, R.A. & Luster, A.D. (2001) SDF-1 alpha induces chemotaxis and enhances sonic hedgehog-induced proliferation of cerebellar granule cells. *Development*, **128**, 1971–1981.

Komuro, H. & Rakic, P. (1995) Dynamics of granule cell migration: a confocal microscopic study in acute cerebellar slice preparations. *J. Neurosci.*, **15**, 1110–1120.

Komuro, H. & Rakic, P. (1996) Intracellular Ca^{2+} fluctuations modulate the rate of neuronal migration. *Neuron*, **17**, 275–285.

Komuro, H., Yacubova, E. & Rakic, P. (2001) Mode and tempo of tangential cell migration in the cerebellar external granular layer. *J. Neurosci.*, **21**, 527–540.

Le Gouill, C., Parent, J.L., Rola-Pleszczynski, M. & Stankova, J. (1997) Structural and functional requirements for agonist-induced internalization of the human platelet-activating factor receptor. *J. Biol. Chem.*, **272**, 21289–21295.

Lindsberg, P.J., Hallenbeck, J.M. & Feuerstein, G. (1991) Platelet-activating factor in stroke and brain injury. *Ann. Neurol.*, **30**, 117–129.

Marcheselli, V.L., Rossowska, M.J., Domingo, M.T., Braquet, P. & Bazan, N.G. (1990) Distinct platelet-activating factor binding sites in synaptic endings and in intracellular membranes of rat cerebral cortex. *J. Biol. Chem.*, **265**, 9140–9145.

Menon, A.K. (1995) Flippases. *Trends Cell Biol.*, **5**, 355–360.

Mori, M., Aihara, M., Kume, K., Hamanoue, M., Kohsaka, S. & Shimizu, T. (1996) Predominant expression of platelet-activating factor receptor in the rat brain microglia. *J. Neurosci.*, **16**, 3590–3600.

Morris, R. (2000) A rough guide to a smooth brain. *Nature Cell Biol.*, **2**, E201–E202.

Nagase, T., Ishii, S., Kume, K., Uozumi, N., Izumi, T., Ouchi, Y. & Shimizu, T. (1999) Platelet-activating factor mediates acid-induced lung injury in genetically engineered mice. *J. Clin. Invest.*, **104**, 1071–1076.

Nagase, T., Uozumi, N., Ishii, S., Kita, Y., Yamamoto, H., Ohga, E., Ouchi, Y. & Shimizu, T. (2002) A pivotal role of cytosolic phospholipase A2 in bleomycin-induced pulmonary fibrosis. *Nature Med.*, **8**, 480–484.

Nagata, I. & Nakatsuji, N. (1990) Granule cell behavior on laminin in cerebellar microexplant cultures. *Brain Res. Dev Brain Res.*, **52**, 63–73.

Nakamura, M., Honda, Z., Izumi, T., Sakanaka, C., Mutoh, H., Minami, M., Bito, H., Seyama, Y., Matsumoto, T., Noma, M. & Shimizu, T. (1991) Molecular cloning and expression of platelet-activating factor receptor from human leukocytes. *J. Biol. Chem.*, **266**, 20400–20405.

Niethammer, M., Smith, D.S., Ayala, R., Peng, J., Ko, J., Lee, M.S., Morabito, M. & Tsai, L.H. (2000) NUDEL is a novel Cdk5 substrate that associates with LIS1 and cytoplasmic dynein. *Neuron*, **28**, 697–711.

O'Flaherty, J.T., Redman, J.F. Jr, Schmitt, J.D., Ellis, J.M., Surles, J.R., Marx, M.H., Piantadosi, C. & Wykle, R.L. (1987) 1-*O*-alkyl-2-*N*-methylcarbamylglycerophosphocholine: a biologically potent, non-metabolizable analog of platelet-activating factor. *Biochem. Biophys. Res. Commun.*, **147**, 18–24.

Ogden, F., DeCoster, M.A. & Bazan, N.G. (1998) Recombinant plasma-type platelet-activating factor acetylhydrolase attenuates NMDA-induced hippocampal neuronal apoptosis. *J. Neurosci. Res.*, **53**, 677–684.

Ohshima, N., Ishii, S., Izumi, T. & Shimizu, T. (2002) Receptor-dependent metabolism of platelet-activating factor in murine macrophages. *J. Biol. Chem.*, **277**, 9722–9727.

Prescott, S.M., Zimmerman, G.A., Stafforini, D.M. & McIntyre, T.M. (2000) Platelet-activating factor and related lipid mediators. *Annu. Rev. Biochem.*, **69**, 419–445.

Reiner, O., Carrozzo, R., Shen, Y., Wehnert, M., Faustinella, F., Dobyns, W.B., Caskey, C.T. & Ledbetter, D.H. (1993) Isolation of a Miller-Dieker lissencephaly gene containing G protein β-subunit-like repeats. *Nature*, **364**, 717–721.

Ryder, E.F. & Cepko, C.L. (1994) Migration patterns of clonally related granule cells and their progenitors in the developing chick cerebellum. *Neuron*, **12**, 1011–1028.

Sasaki, S., Shionoya, A., Ishida, M., Gambello, M.J., Yingling, J., Wynshaw-Boris, A. & Hirotsune, S. (2000) A LIS1/NUDEL/cytoplasmic dynein heavy chain complex in the developing and adult nervous system. *Neuron*, **28**, 681–696.

Snyder, F. (1995) Platelet-activating factor: the biosynthetic and catabolic enzymes. *Biochem. J.*, **305**, 689–705.

Strømgaard, K., Saito, D.R., Shindou, H., Ishii, S., Shimizu, T. & Nakanishi, K. (2002) Ginkgolide derivatives for photolabeling studies: preparation and pharmacological evaluation. *J. Med. Chem.*, **45**, 4038–4046.

Sweeney, K.J., Clark, G.D., Prokscha, A., Dobyns, W.B. & Eichele, G. (2000) Lissencephaly associated mutations suggest a requirement for the PAFAH1B heterotrimeric complex in brain development. *Mech. Dev*, **92**, 263–271.

Talley, A.K., Dewhurst, S., Perry, S.W., Dollard, S.C., Gummuluru, S., Fine, S.M., New, D., Epstein, L.G., Gendelman, H.E. & Gelbard, H.A. (1995) Tumor necrosis factor alpha-induced apoptosis in human neuronal cells: protection by the antioxidant *N*-acetylcysteine and the genes *bcl-2* and *crmA*. *Mol. Cell Biol.*, **15**, 2359–2366.

Tjoelker, L.W., Wilder, C., Eberhardt, C., Stafforini, D.M., Dietsch, G., Schimpf, B., Hooper, S., Le Trong, H., Cousens, L.S., Zimmerman, G.A., Yamada, Y., McIntyre, T.M., Prescott, S.M. & Gray, P.W. (1995) Anti-inflammatory properties of a platelet-activating factor acetylhydrolase. *Nature*, **374**, 549–553.

Tong, N., Sanchez, J.F., Maggirwar, S.B., Ramirez, S.H., Guo, H., Dewhurst, S. & Gelbard, H.A. (2001) Activation of glycogen synthase kinase 3 beta (GSK-3β) by platelet activating factor mediates migration and cell death in cerebellar granule neurons. *Eur. J. Neurosci.*, **13**, 1913–1922.

Wu, C., Stojanov, T., Chami, O., Ishii, S., Shimuzu, T., Li, A. & O'Neill, C. (2001) Evidence for the autocrine induction of capacitation of mammalian spermatozoa. *J. Biol. Chem.*, **276**, 26962–26968.

Wynshaw-Boris, A. & Gambello, M.J. (2001) LIS1 and dynein motor function in neuronal migration and development. *Genes Dev.*, **15**, 639–651.

Yacubova, E. & Komuro, H. (2002) Stage-specific control of neuronal migration by somatostatin. *Nature*, **415**, 77–81.

Yamasaki, T., Kawaji, K., Ono, K., Bito, H., Hirano, T., Osumi, N. & Kengaku, M. (2001) Pax6 regulates granule cell polarization during parallel fiber formation in the developing cerebellum. *Development*, **128**, 3133–3144.

Yue, T.L. & Feuerstein, G.Z. (1994) Platelet-activating factor: a putative neuromodulator and mediator in the pathophysiology of brain injury. *Crit. Rev. Neurobiol.*, **8**, 11–24.

Yue, T.L., Lysko, P.G. & Feuerstein, G. (1990) Production of platelet-activating factor from rat cerebellar granule cells in culture. *J. Neurochem.*, **54**, 1809–1811.

THE JOURNAL OF BIOLOGICAL CHEMISTRY
Vol. 278, No. 28, Issue of July 11, pp. 25600–25606, 2003
Printed in U.S.A.

Identification of p2y$_9$/GPR23 as a Novel G Protein-coupled Receptor for Lysophosphatidic Acid, Structurally Distant from the Edg Family*

Received for publication, March 14, 2003, and in revised form, April 28, 2003
Published, JBC Papers in Press, April 30, 2003, DOI 10.1074/jbc.M302648200

Kyoko Noguchi, Satoshi Ishii‡, and Takao Shimizu

From the Department of Biochemistry and Molecular Biology, Faculty of Medicine, The University of Tokyo, Core Research for Evolutional Science and Technology (CREST) of Japan Science and Technology Corporation, Hongo, Bunkyo-ku, Tokyo 113-0033, Japan

Lysophosphatidic acid (LPA) is a bioactive lipid mediator with diverse physiological and pathological actions on many types of cells. LPA has been widely considered to elicit its biological functions through three types of G protein-coupled receptors, Edg-2 (endothelial cell differentiation gene-2)/LPA$_1$/vzg-1 (ventricular zone gene-1), Edg-4/LPA$_2$, and Edg-7/LPA$_3$. We identified an orphan G protein-coupled receptor, p2y$_9$/GPR23, as the fourth LPA receptor (LPA$_4$). Membrane fractions of RH7777 cells transiently expressing p2y$_9$/GPR23 displayed a specific binding for 1-oleoyl-LPA with a K_d value of around 45 nM. Competition binding and reporter gene assays showed that p2y$_9$/GPR23 preferred structural analogs of LPA with a rank order of 1-oleoyl- > 1-stearoyl- > 1-palmitoyl- > 1-myristoyl- > 1-alkyl- > 1-alkenyl-LPA. In Chinese hamster ovary cells expressing p2y$_9$/GPR23, 1-oleoyl-LPA induced an increase in intracellular Ca^{2+} concentration and stimulated adenylyl cyclase activity. Quantitative real-time PCR demonstrated that mRNA of p2y$_9$/GPR23 was significantly abundant in ovary compared with other tissues. Interestingly, p2y$_9$/GPR23 shares only 20–24% amino acid identities with Edg-2/LPA$_1$, Edg-4/LPA$_2$, and Edg-7/LPA$_3$, and phylogenetic analysis also shows that p2y$_9$/GPR23 is far distant from the Edg family. These facts suggest that p2y$_9$/GPR23 has evolved from different ancestor sequences from the Edg family.

Lysophosphatidic acid (LPA, 1- or 2-acyl-*sn*-glycero-3-phosphate)[1] is a bioactive phospholipid with diverse physiological actions on many cell types (1, 2). LPA induces mitogenic and/or morphological effects on the cells and has been proposed to be involved in biologically important processes, including neurogenesis, myelination, angiogenesis, wound healing, and cancer progression (1, 3). LPA is present in serum at micromolar concentrations (4). LPA is generated mainly by two different pathways; 1) generation of lysophospholipids such as lysophosphatidylcholine (LPC), lysophosphatidylethanolamine (LPE), and lysophosphatidylserine (LPS) from membrane phospholipids by phospholipase A$_2$ (PLA$_2$) or phospholipase A$_1$, followed by conversion of these lysophospholipids to LPA by lysophospholipase D (5) and 2) generation of phosphatidic acid (PA) from phosphatidylcholine (PC) by phospholipase D, followed by conversion of PA to LPA by specific classes of PLA$_2$ (6).

It has been demonstrated that cell-surface G protein-coupled receptors mediate the cellular effects of LPA. At least three types of G protein-coupled receptors, Edg-2/LPA$_1$/vzg-1 (7), Edg-4/LPA$_2$ (8), and Edg-7/LPA$_3$ (9), which belong to the Edg (endothelial cell differentiation gene) family, have been identified as specific receptors for LPA. These three G protein-coupled receptors share 50–57% amino acid identities. Several experiments have demonstrated that they can mediate adenylyl cyclase inhibition, mitogen-activated protein kinase activation, phospholipase C activation, and Ca^{2+} mobilization through pertussis toxin-sensitive ($G_{i/o}$) and -insensitive G proteins ($G_{12/13}$ and $G_{q/11/14}$) (2, 3). Edg-4/LPA$_2$ and Edg-7/LPA$_3$ have also been shown to activate adenylyl cyclase when they were overexpressed in Sf9 insect cells (9). However, the existence of one or more additional LPA receptors has been implied from the analysis of Edg-2/LPA$_1^{(-/-)}$ Edg-4/LPA$_2^{(-/-)}$ double knockout mice (10) and various pharmacological studies (11–13).

During a "de-orphaning" project of G protein-coupled receptors, we found that p2y$_9$/GPR23 responded to LPA. p2y$_9$/GPR23 specifically bound to LPA and mediated LPA-induced adenylyl cyclase stimulation and intracellular Ca^{2+} mobilization. Although p2y$_9$/GPR23 shares only 20–24% amino acid identities with Edg-2/LPA$_1$, Edg-4/LPA$_2$, and Edg-7/LPA$_3$, and the phylogenetic analysis also shows that p2y$_9$/GPR23 is distant from the Edg family (Fig. 1), our results consistently indicate that p2y$_9$/GPR23 is the fourth LPA receptor (LPA$_4$).

EXPERIMENTAL PROCEDURES

Materials and Cells—1-Myristoyl (14:0), -palmitoyl (16:0), -stearoyl (18:0), and -oleoyl (18:1)-LPAs, 18:1-LPC, 18:1-LPE, 18:1-lysophosphatidylglycerol (LPG), and 18:1-LPS were purchased from Avanti Polar Lipids (Alabaster, AL). 18:1-LPA was also purchased from Cayman

* This work was supported by grants-in-aid from the Ministry of Education, Science, Culture, Sports and Technology of Japan (to T. S. and S. I.), grants-in-aid for Comprehensive Research on Aging and Health, and Research on Allergic Disease and Immunology from the Ministry of Health, Labour, and Welfare, Japan, and grants from the Yamanouchi Foundation for Research on Metabolic Disorders, the Kanae Foundation for Life and Socio-medical Science, and the Uehara Memorial Foundation (to S. I.). The costs of publication of this article were defrayed in part by the payment of page charges. This article must therefore be hereby marked "*advertisement*" in accordance with 18 U.S.C. Section 1734 solely to indicate this fact.

‡ To whom correspondence should be addressed. Tel.: 81-3-5802-2925; Fax: 81-3-3813-8732; E-mail: mame@m.u-tokyo.ac.jp.

[1] The abbreviations used are: LPA, lysophosphatidic acid; LPC, lysophosphatidylcholine; LPE, lysophosphatidylethanolamine; LPS, lysophosphatidylserine; PLA$_2$, phospholipase A$_2$; PA, phosphatidic acid; PC, phosphatidylcholine; 14:0, 1-myristoyl; 16:0, 1-palmitoyl; 18:0, 1-stearoyl; 18:1, 1-oleoyl; LPG, lysophosphatidylglycerol; PAF, platelet-activating factor; S1P, sphingosine 1-phosphate; SPC, sphingosylphosphorylcholine; BSA, bovine serum albumin; DMEM, Dulbecco's modified Eagle's medium; HA, hemagglutinin; CHO, Chinese hamster ovary; HBSS, Hanks' balanced salt solution; $[Ca^{2+}]_i$, intracellular Ca^{2+} concentration; GAPDH, glyceraldehyde-3-phosphate dehydrogenase; EST, expressed sequence tag.

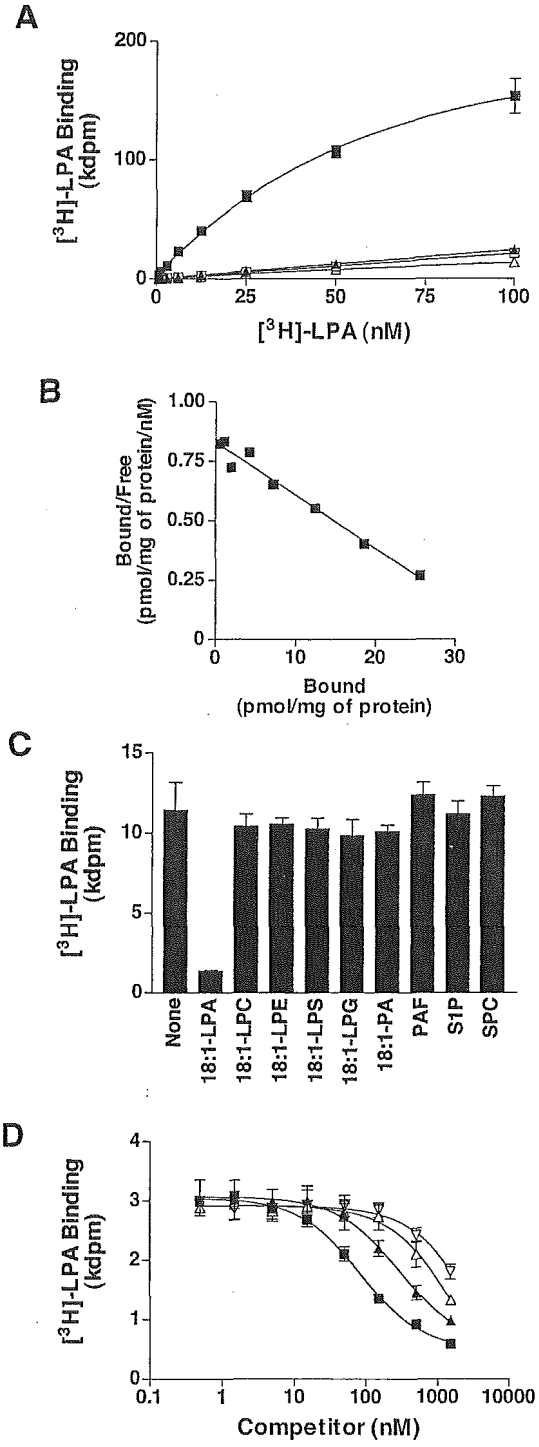

FIG. 2. **[^{3}H]LPA binding to RH7777 cell membranes.** *A*, [^{3}H]LPA binding to p2y$_9$/GPR23. Membrane fractions of RH7777 cells transiently expressing p2y$_9$/GPR23 (*closed symbols*) and mock-transfected cells (*open symbols*) were incubated with increasing concentrations of [^{3}H]18:1-LPA in the presence or absence of 10 μM unlabeled 18:1-LPA. Total binding (■ and □) and nonspecific binding (▲ and △) are presented. Data are means ± S.D. (n = 3). *B*, Scatchard analysis of the specific binding of [^{3}H]LPA to p2y$_9$/GPR23. *C*, competition for [^{3}H]LPA binding with related lipids. Membrane fractions of RH7777 cells transiently expressing p2y$_9$/GPR23 were incubated with 5 nM [^{3}H]18:1-LPA in the presence of 1 μM unlabeled lipids. The total amounts of [^{3}H]LPA bound are presented. Data are means ± S.D. (n = 3) of a representative of two independent experiments. *D*, competition for [^{3}H]LPA binding with structural analogs of LPA. Membrane fractions of RH7777 cells transiently expressing p2y$_9$/GPR23 were incubated with increasing concentrations of unlabeled 18:1- (■), 18:0- (▲), 1-alkyl- (△), and 1-alkenyl- (▽) LPA in the presence of 2.5 nM [^{3}H]18:1-LPA. The total amounts of [^{3}H]LPA bound are presented. Data are means ± S.D. (n = 3) of a representative of two independent experiments.

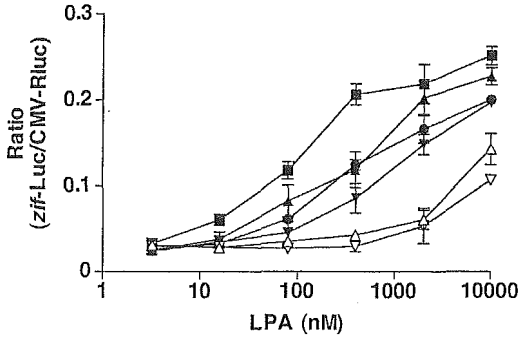

FIG. 3. **Induction of reporter gene expression by structural analogs of LPA in PC-12 cells.** PC-12 cells were transiently transfected with the reporter plasmids containing the *zif* 268 promoter-driven firefly luciferase gene and the control plasmid containing the cytomegalovirus promoter-driven *Renilla* luciferase gene together with the p2y$_9$/GPR23 expression plasmid. Cells were stimulated with increasing concentrations of 18:1- (■), 18:0- (▲), 16:0- (●), 14:0- (▼), 1-alkyl- (△), and 1-alkenyl- (▽) LPA. The ratios of firefly luciferase activity to *Renilla* one are shown. Data are means ± S.D. (n = 3) of a representative of two independent experiments.

observed, using different batches of the LPA from two companies (Cayman and Avanti). In B103 cells transiently expressing p2y$_9$/GPR23, 18:1-LPA at concentrations of 1 and 10 nM evoked increases in $[Ca^{2+}]_i$ by 38 ± 5 and 49 ± 5 nM (mean ± S.D.; n = 3), respectively. Mock-transfected B103 cells showed no response at 10 nM 18:1-LPA. On the other hand, RH7777 cells were unresponsive to 18:1-LPA both in mock-transfected and in p2y$_9$/GPR23-expressing form (data not shown).

Effect on cAMP Formation—18:1-LPA induced an increase in cAMP levels in p2y$_9$/GPR23-expressing CHO cells either in the absence or presence of 5 μM forskolin (Fig. 5, *A* and *B*), and pretreatment of the cells with pertussis toxin further increased the cAMP levels (Fig. 5, *A* and *B*). In mock-transfected CHO cells, LPA induced no change or a decrease in cAMP levels in the absence or presence of forskolin, respectively (Fig. 5, *A* and *B*), and pretreatment of the cells with pertussis toxin attenuated an LPA-induced decrease in cAMP levels (Fig. 5*B*).

Tissue Distribution—To explore the physiological function of p2y$_9$/GPR23 *in vivo*, it is important to know the tissue distribution of the receptor. By using cDNAs prepared from 16 human tissues as templates, quantitative real-time PCR was performed to estimate the mRNA expression levels. In a set of samples, ovary showed the highest expression of p2y$_9$/GPR23 mRNA, whereas other tissues showed only weak expressions (Fig. 6*A*). Northern hybridization of human poly(A)$^+$ RNA from kidney, skeletal muscle, and megakaryoblastic MEG-01 cells (20) detected a transcript of about 4.4 kb (Fig. 6*C*).

DISCUSSION

LPA is a lipid mediator with diverse physiological activities (1, 3). Many structural analogs of LPA have been identified in mammalian cells and tissues. Most are 1-acyl-LPAs with unsaturated fatty acyl-chains (oleoyl, linoleoyl, and arachidonoyl), and smaller amounts are with saturated fatty acyl-chains (palmitoyl and stearoyl) (21). Recently, 1-alkyl-, 1-alkenyl-, and 2-acyl-LPAs were also found (22–24). LPA has been widely considered to elicit its physiological functions through three types of G protein-coupled receptors, Edg-2/LPA$_1$, Edg-4/LPA$_2$, and Edg-7/LPA$_3$ (2, 3). However, there are some reports implying the existence of an additional LPA receptor(s). First, in the study of Edg-2/LPA$_1^{(-/-)}$ Edg-4/LPA$_2^{(-/-)}$ double knockout mice, some LPA-induced responses, such as inositol phosphate production, adenylyl cyclase inhibition, and stress fiber formation, were absent or severely reduced but still remained at high LPA concentrations in embry-

Chemical (Ann Arbor, MI). 1-Alkyl- and 1-alkenyl-LPAs were kind gifts from Dr. R. Taguchi (Nagoya City University, Japan), which were prepared from bovine heart lyso-platelet-activating factor (lyso-PAF) and lyso-plasmalogen, respectively, by using phospholipase D. 18:1-PA and 17 nucleotides (ADP-glucose, ATP, ADP, *S*-adenosyl-L-methionine, *S*-adenosyl-L-homocysteine, CTP, GDP-fucose, GDP-mannose, GDP, UDP, UDP-*N*-acetylglucosamine, UDP-galactose, UDP-glucose, UDP-*N*-acetylgalactosamine, UTP, UDP-glucuronic acid, and GTP) were from Sigma (St. Louis, MO). Sphingosine 1-phosphate (S1P) and the Bioactive Lipid Library were from Biomol Research Laboratories (Plymouth Meeting, PA). Sphingosylphosphorylcholine (SPC) and 1-*O*-hexadecyl-PAF were from Cayman Chemical. [^{3}H]LPA (1-oleoyl[oleoyl-9,10-^{3}H(N)]LPA, 57 Ci/mmol) was from PerkinElmer Life Sciences (Boston, MA). Bovine serum albumin (BSA) from Serologicals Proteins (Kankakee, IL) was of fatty acid-free and very low endotoxin grade. Other chemical reagents were of analytical grade. RH7777 rat hepatoma cells and B103 rat neuroblastoma cells were kindly provided from Dr. J. Chun (University of California-San Diego, La Jolla, CA). Human megakaryoblastic MEG-01 cells were purchased from the Health Science Research Resources Bank (Osaka, Japan).

Construction of the Phylogenetic Tree—Peptide sequences of selected G protein-coupled receptors were obtained from GenBank™ and SwissProt. The phylogenetic tree was generated from peptide sequences of selected G protein-coupled receptors, using the all-against-all matching method (available at cbrg.inf.ethz.ch/Server/AllAll.html). The tree was constructed on the basis of point-accepted mutation distances between each pair of sequences estimated by the dynamic programming algorithm.

Cloning of p2y$_9$/GPR23—The tBLASTn program was used to search the data base of GenBank™ for orphan G protein-coupled receptors sharing high identities with the human PAF receptor (14). A DNA fragment containing the entire open reading frame of p2y$_9$/GPR23 (GenBank™ accession number NM_005296) was first amplified from human genomic DNA by PCR using KOD-Plus (Toyobo, Osaka, Japan) and oligonucleotides (sense primer, 5′-GTCCATAGTGTCAGAGTGGTGAAC-3′; antisense primer, 5′-CATATCTGGACCTGAACACATTTC-3′). The entire open reading frame of p2y$_9$/GPR23 with an additional sequence of hemagglutin (HA)-epitope at the 5′-end was subsequently amplified from the resultant PCR products using KOD-Plus and oligonucleotides (sense primer containing *Kpn*I and HA tag sequences, 5′-GGGGTACCGCCATGTACCCCTACGACGTGCCCGACTACGCCGGTGACAGAAGATTCATT-3′; antisense primer containing *Xba*I sequence, 5′-GCTCTAGACTAAAAGGTGGATTCTAG-3′). The resultant DNA fragment was digested with *Kpn*I and *Xba*I and subsequently cloned into the mammalian expression vector pCXN2.1, a slightly modified version of pCXN2 (15) with multiple cloning sites, between *Kpn*I and *Nhe*I sites.

Binding Assay—RH7777 cells and B103 cells were cultured on collagen-coated dishes in Dulbecco's modified Eagle's medium (DMEM, Sigma) supplemented with 10% fetal bovine serum (Cambrex Co., Walkersville, MD), 100 IU/ml penicillin, and 100 μg/ml streptomycin (Roche Applied Science). Cells were transfected with p2y$_9$/GPR23-pCXN2.1 or empty vector using LipofectAMINE 2000 reagent (Invitrogen). After 24 h of transfection, cells were washed with phosphate-buffered saline three times and serum-starved for 24 h in DMEM supplemented with 0.1% BSA. The cells were washed again with phosphate-buffered saline twice and scraped off. After further washing with binding buffer (25 mM HEPES-NaOH (pH 7.4), 10 mM $MgCl_2$, and 0.25 M sucrose), the cells were suspended in the buffer with additional 20 μM 4-amidinophenylmethylsulfonyl fluoride (Sigma) and a protease inhibitor mixture (Complete, Roche Applied Science), sonicated three times at 15 watts for 30 s, and centrifuged at 800 × *g* for 10 min at 4 °C. The supernatant was further centrifuged at 10^5 × *g* for 60 min at 4 °C, and the resultant pellet was homogenized in ice-cold binding buffer. Binding assays were performed in 96-well plates in triplicates. For Scatchard analysis, 40 μg of the membrane fractions were incubated in binding buffer containing 0.25% BSA with various concentrations of [^{3}H]LPA for 60 min at 4 °C. The bound [^{3}H]LPA was collected onto a Unifilter-96-GF/C (PerkinElmer Life Sciences) using a MicroMate 196 harvester (Packard, Wellesley, MA). The filter was then rinsed ten times with binding buffer containing 0.25% BSA and dried for 2 h at 50 °C. 25 μl of MicroScint-0 scintillation mixture (PerkinElmer Life Sciences) was added per well. The radioactivity that remained on the filter was measured with a TopCount microplate scintillation counter (Packard). Total and nonspecific bindings were evaluated in the absence and presence of 10 μM unlabeled LPA, respectively. The specific binding value (dpm) was calculated by subtracting the nonspecific binding value (dpm) from the total binding value (dpm). For competition assay with related lipids, 20 μg of the membrane fractions were incubated with 5 nM [^{3}H]LPA in the absence or presence of 1 μM of unlabeled 18:1-LPA, 18:1-LPC, 18:1-LPE, 18:1-LPS, 18:1-LPG, 18:1-PA, PAF, S1P, or SPC. For competition assay with structural analogs of LPA, 10 μg of the membrane fractions was incubated with increasing concentrations of unlabeled 18:1-, 18:0-, 1-alkyl-, and 1-alkenyl-LPA in the presence of 2.5 nM [^{3}H]LPA. Before conducting the binding assays, the cell surface expression of p2y$_9$/GPR23 was confirmed by flow cytometric analysis (Epics XL, Beckman Coulter, Fullerton, CA) with anti-HA rat IgG (3F10, Roche Applied Science) and phycoerythrin-labeled anti-rat IgG (Beckman Coulter) as the second antibody.

Reporter Gene Assay—PC-12 cells were cultured in DMEM supplemented with 10% horse serum and 5% fetal bovine serum. 2 × 10^5 cells were transfected with 450 ng of p2y$_9$/GPR23-pCXN2.1 or empty vector, 530 ng of *zif* 268-firefly luciferase-pGL2 (a kind gift from Dr. T. Naito, Japan Tobacco, Tokyo, Japan), and 20 ng of CMV-*Renilla* luciferase-pRL (Promega, Madison, WI) using SuperFect (Qiagen, Hiden, Germany), and cultured on collagen-coated 24-well plates for 48 h. Cells were washed three times with DMEM supplemented with 0.1% BSA and cultured in the serum-free DMEM for 12 h, and stimulated with various concentrations of LPA analogs. Firefly and *Renilla* luciferase activities were measured using PICAGENE Dual Seapansy (Toyo Ink, Tokyo, Japan) and a MiniLumat LB 9506 luminometer (Berthold, Bundoora, Australia). Firefly luciferase values were standardized to *Renilla* ones.

Ca^{2+} Measurement—Chinese hamster ovary (CHO) cells were cultured in Ham's F-12 (Sigma) supplemented with 10% fetal bovine serum, 100 IU/ml penicillin, and 100 μg/ml streptomycin. Cells were transfected with p2y$_9$/GPR23-pCXN2.1 or empty vector using LipofectAMINE 2000 reagent. Stably transfected clones were selected with 2 mg/ml G418 (Invitrogen, Carlsbad, CA) and maintained with 0.3 mg/ml G418. Cell surface expression of p2y$_9$/GPR23 was detected by flow cytometric analysis as described above (see Fig. 4*A*). For the ligand screening assay, clones highly expressing p2y$_9$/GPR23 were seeded in 96-well plates at a density of 4 × 10^4 cells/well and cultured overnight. They were loaded with 4 μM Fluo-3 AM (Dojindo, Kumamoto, Japan) in HEPES-HBSS buffer (1 × Hanks' balanced salt solution (HBSS) containing 20 mM HEPES-NaOH (pH 7.4), 1 mM $CaCl_2$, 0.5 mM $MgCl_2$, 0.1% BSA, and 2.5 mM probenecid) and 0.04% pluronic acid for 1 h at 37 °C, washed twice, and filled with HEPES-HBSS buffer. They were then stimulated with 198 lipids contained in the Bioactive Lipid Library and 17 nucleotides (described under "Materials and Cells") individually, and intracellular Ca^{2+} mobilization was monitored with a scanning fluorometer (FLEXstation, Molecular Devices, Sunnyvale, CA) at an excitation wavelength of 485 nm and an emission wavelength of 525 nm. For examination of dose dependence, CHO cell clones highly expressing p2y$_9$/GPR23 or mock-transfected cells were washed with phosphate-buffered saline three times, serum-starved for 24 h in Ham's F-12 supplemented with 0.1% BSA, washed twice again with phosphate-buffered saline, and then harvested. The harvested cells were further washed with HEPES-Tyrode's buffer (25 mM HEPES-NaOH (pH 7.4), 140 mM NaCl, 2.7 mM KCl, 1 mM $CaCl_2$, 0.49 mM $MgCl_2$, 12 mM $NaHCO_3$, 0.37 mM NaH_2PO_4, and 5.6 mM D-glucose), and loaded with 3 μM Fura-2 AM (Dojindo) in HEPES-Tyrode's buffer containing 0.1% BSA (HEPES-Tyrode's BSA buffer) for 1 h at 37 °C. Cells were washed twice and resuspended in HEPES-Tyrode's BSA buffer at a density of 2 × 10^6 cells/ml. 0.5 ml of the cell suspension was applied to a CAF-100 spectrofluorometer (Jasco, Tokyo, Japan), and 5 μl of various concentrations of 18:1-LPA in HEPES-Tyrode's BSA buffer was added. Intracellular Ca^{2+} concentration ($[Ca^{2+}]_i$) was measured by the ratio of emission fluorescence of 500 nm by excitations at 340 and 380 nm.

cAMP Assay—CHO cell clones stably expressing p2y$_9$/GPR23 were used to measure cAMP levels. After 24 h of serum starvation, cells were harvested and suspended in HBSS containing 0.1% BSA and 0.5 mM isobutylmethylxanthine. The density was 5 × 10^6 or 5 × 10^7 cells/ml for assay in the presence or absence of forskolin, respectively. 20 μl of the cell suspension was applied to 96-well plates and incubated for 20 min at room temperature. The reaction was initiated by adding 10 μl of ligand solution of 18:1-LPA in HBSS-BSA buffer with or without 5 μM forskolin. After 30 min of incubation at room temperature, the reaction was terminated by adding 10 μl of HBSS-BSA buffer containing 4% Tween 20. After centrifugation at 800 × *g* for 5 min, cAMP contents in the supernatant were measured by a Fusion system (Packard) using an AlphaScreen cAMP assay kit (PerkinElmer Life Sciences). Pretreatment with pertussis toxin (List Biological Laboratories, Campbell, CA) was for 12 h at a concentration of 100 ng/ml. Results were expressed as -fold increases over respective controls.

Quantitative Real-time PCR—Human first strand cDNAs from 16 tissues were purchased from Clontech (Human MTC Panel I and II),

whose concentrations were normalized to the mRNA expression levels of four different housekeeping genes (α-tubulin, β-actin, glyceraldehyde-3-phosphate dehydrogenase (GAPDH), and PLA_2). The cDNA levels of GAPDH and $p2y_9$/GPR23 were quantified using a LightCycler apparatus (Roche Applied Science). The PCR reactions were set up in microcapillary tubes in a volume of 20 μl, consisting of 2 μl of cDNA solution, 1× FastStart DNA Master SYBR Green I (Roche Applied Science), 0.5 μM each sense and antisense primers and 3 mM $MgCl_2$. The PCR program for GAPDH was as follows; denaturation at 95 °C for 3 min and 50 cycles of amplification consisting of denaturation at 95 °C for 0 s, annealing at 60 °C for 5 s, and extension at 72 °C for 40 s. The PCR program for $p2y_9$/GPR23 was as follows: denaturation at 95 °C for 5 min and 50 cycles of amplification consisting of denaturation at 95 °C for 15 s, annealing at 60 °C for 5 s, and extension at 72 °C for 6 s. For GAPDH, a human GAPDH control Amplimer Set (Clontech), designed to amplify a 983-bp fragment was used as primers; sense primer: 5′-TGAAGGTCGGAGTCAACGGATTTGGT-3′ and antisense primer: 5′-CATGTGGGCCATGAGGTCCACCAC-3′. The primers for $p2y_9$/GPR23 were designed to amplify a 139-bp fragment; sense primer: 5′-AAAGATCATGTACCCAATCACCTT-3′ and antisense primer: 5′-CTTAAACAGGGACTCCATTCTGAT-3′. The PCR products were detected by measuring the fluorescence of SYBR Green I, which selectively bound to double-stranded DNA and emitted the greatly enhanced fluorescence. The cDNA level of each sample was quantified by Fit Points Method in LightCycler analysis software. The control cDNA contained in Clontech human MTC Panels and a linearized $p2y_9$/GPR23-pCXN2.1 were used as standards for GAPDH and $p2y_9$/GPR23, respectively. In both cases, the quality of PCR products was assessed by monitoring a fusion step.

Northern Hybridization—Human poly(A)$^+$ RNA samples from kidney and skeletal muscle were purchased from Clontech. Total RNA of human megakaryoblastic MEG-01 cells was extracted with Absolutely RNA RT-PCR Miniprep kit (Stratagene, La Jolla, CA). Poly(A)$^+$ RNA was isolated from 200 μg of the total RNA using μMACS mRNA isolation kit (Miltenyi Biotec, Bergisch Gladbach, Germany). For Northern analysis, 2.5 μg of poly(A)$^+$ RNA was hybridized with [^{32}P]dCTP-labeled probes of human $p2y_9$/GPR23 and human β-actin, as described previously (16). The washed membrane was subjected to autoradiography for 4 days ($p2y_9$/GPR23) or 3 h (β-actin).

RESULTS

Screening of Candidate Ligands—Phylogenetic analysis showed that $p2y_9$/GPR23 was most closely related to the orphan receptor $p2y_5$ and relatively close to the functional receptors for nucleotides ($P2Y_1$, $P2Y_4$, and $P2Y_6$) (17) and for lipids (G2A, GPR4, GPR65/TDAG8, GPR68/OGR1, PAF receptor, $CysLT_1$, and $CysLT_2$) (18) (Fig. 1). It was, therefore, supposed that $p2y_9$/GPR23 might interact with lipids or nucleotides. We screened 198 lipids and 17 nucleotides using CHO cells stably expressing $p2y_9$/GPR23 by measuring intracellular Ca^{2+} mobilization with FLEXstation, a scanning fluorometer. Among them, 18:1-LPA at a concentration of 10 μM induced a significant increase in $[Ca^{2+}]_i$ in $p2y_9$/GPR23-expressing cells, but not in $p2y_5$-expressing cells (data not shown).

Membrane Binding Assay—To characterize the binding of LPA to $p2y_9$/GPR23, we conducted membrane binding assays using [^{3}H]18:1-LPA. RH7777 rat hepatoma cells transiently transfected with $p2y_9$/GPR23 were used, because RH7777 cells were not responsive to LPA (19). As expected, membrane fractions of mock-transfected RH7777 cells displayed low background binding of [^{3}H]LPA (Fig. 2*A*). [^{3}H]LPA binding to membrane fractions of RH7777 cells was greatly enhanced by $p2y_9$/GPR23 transfection (Fig. 2*A*). Reverse transcriptase-PCR analyses showed no induction of endogenous receptors (Edg-2/LPA_1, Edg-4/LPA_2, or Edg-7/LPA_3) by $p2y_9$/GPR23 transfection (data not shown). Scatchard analysis indicated a dissociation constant (K_d) of 44.8 nM and a maximum binding capacity (B_{max}) of 37.2 pmol/mg of protein (Fig. 2*B*). Competition analyses revealed that only 18:1-LPA, but not 18:1-LPC, 18:1-LPE, 18:1-LPS, 18:1-LPG, 18:1-PA, PAF, S1P, or SPC competed for [^{3}H]LPA binding to the membrane fractions of $p2y_9$/GPR23-expressing RH7777 cells (Fig. 2*C*). 18:1- and 18:0-LPA competed for [^{3}H]LPA binding to the membrane fractions of $p2y_9$/GPR23-expressing RH7777 cells with K_i values of 80.0 and 282 nM, respectively (Fig. 2*D*). 1-Alkyl- and 1-alkenyl-LPA also competed for [^{3}H]LPA binding but rather weakly (Fig. 2*D*). Because B103 rat neuroblastoma cells were also reported to lack responsiveness to LPA (19), binding assays using B103 cells were performed in the same manner as RH7777 cells. The specific binding activities of $p2y_9$/GPR23-transfected B103 cells were 289, 859, and 2975 dpm/50 μg of protein at 1, 3, and 10 nM [^{3}H]LPA, respectively. Based on the specific activity of [^{3}H]LPA, 2975 dpm/50 μg of protein corresponds to 0.47 pmol/mg of protein. The binding activities of the mock-transfected B103 cells were 79, 197, and 238 dpm/50 μg of protein at 1, 3, and 10 nM [^{3}H]LPA, respectively.

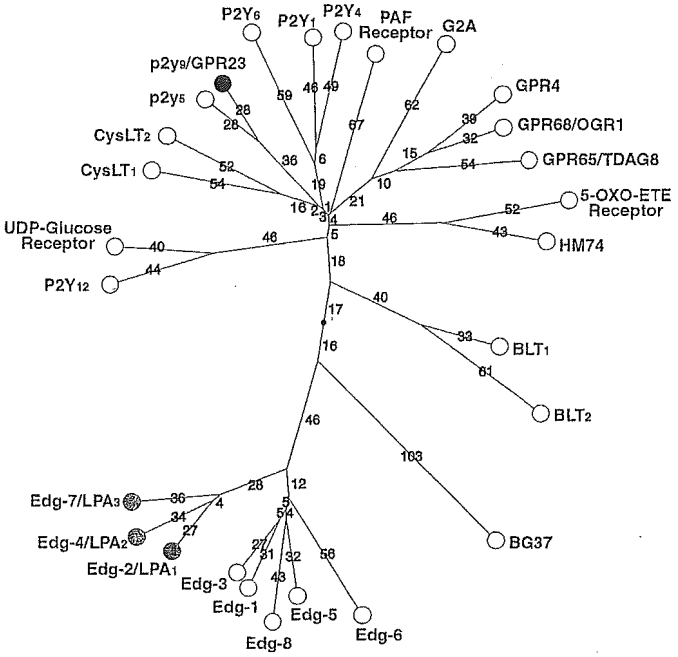

FIG. 1. **Phylogenetic tree constructed for $p2y_9$/GPR23 and selected human G protein-coupled receptors.** Values show branch lengths that represent the evolutionary distance between each pair of sequences. The sequence divergence is equal to the sum of each value of branch length. A *small dot* indicates the weighted centroid of the tree.

Reporter Gene Assay—We next performed reporter gene assays to examine the ligand preference of $p2y_9$/GPR23. The transfected PC-12 cells responded to all LPA analogs with a significant increase in the luciferase activity in a dose-dependent manner; 18:1-LPA evoked the highest activity, followed by 18:0-, 16:0-, and 14:0-derivatives (Fig. 3). Compared with 1-acyl-LPAs, 1-alkyl-, and 1-alkenyl-LPA exhibited weaker activities. Mock-transfected PC-12 cells showed no responses to any analogs of LPA (data not shown).

Effect on Intracellular Ca^{2+} Mobilization—To characterize the intracellular signals of $p2y_9$/GPR23, the effect of LPA on intracellular Ca^{2+} mobilization was examined in detail using a CAF-100 spectrofluorometer. We established four independent clones of CHO cells stably expressing $p2y_9$/GPR23 and a polyclonal population of mock-transfected CHO cells. Cell surface expression of $p2y_9$/GPR23 was confirmed by flow cytometric analysis (Fig. 4*A*). The other three clones showed similar expression patterns. Either in $p2y_9$/GPR23-expressing or mock-transfected CHO cells, 18:1-LPA induced an increase in $[Ca^{2+}]_i$ in a dose-dependent manner (Fig. 4*B*). Although mock-transfected CHO cells displayed a significant increase in $[Ca^{2+}]_i$, the increase in $[Ca^{2+}]_i$ was enhanced ~2-fold by the stable expression of $p2y_9$/GPR23. Similar results were obtained in all four different clones. The effects of 18:1-LPA were reproducibly

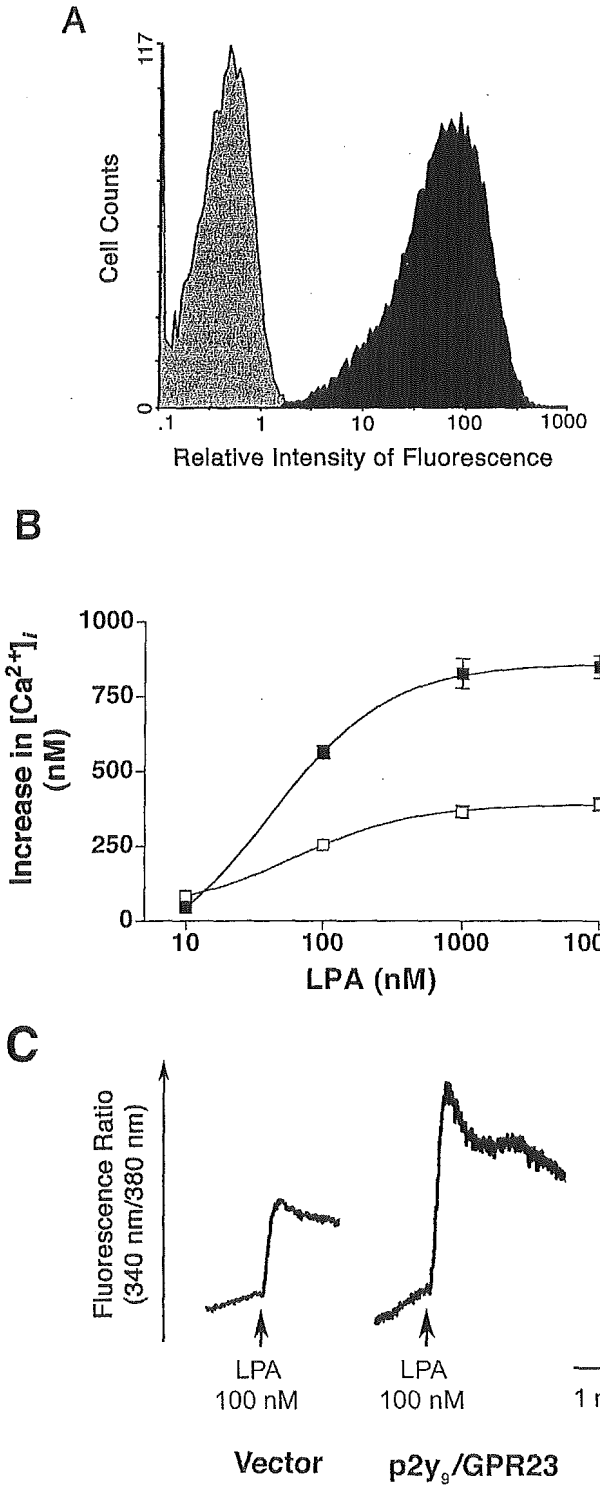

FIG. 4. **LPA-induced increase in $[Ca^{2+}]_i$ in CHO cells.** *A*, cell surface expression of $p2y_9$/GPR23. In a clonal population of CHO cells stably expressing $p2y_9$/GPR23 tagged with HA at N terminus (*black area*), the higher intensity of fluorescence was detected by flow cytometric analysis than in mock-transfected CHO cells (*gray area*). This is a representative result of four independent clones, which gave essentially identical patterns. *B*, dose-response curves. A clonal population of CHO cells stably expressing $p2y_9$/GPR23 was loaded with 3 μM Fura-2 AM, and stimulated with increasing concentrations of 18:1-LPA (■). The results of mock-transfected CHO cells are also shown as a negative control (□). Data are means ± S.D. (n = 3) of a representative of four different stable clones. *C*, representative traces of Ca^{2+} responses. A clonal population of CHO cells stably expressing $p2y_9$/GPR23 was stimulated with 100 nM 18:1-LPA (*right*). A result of mock-transfected CHO cells is also shown as a negative control (*left*).

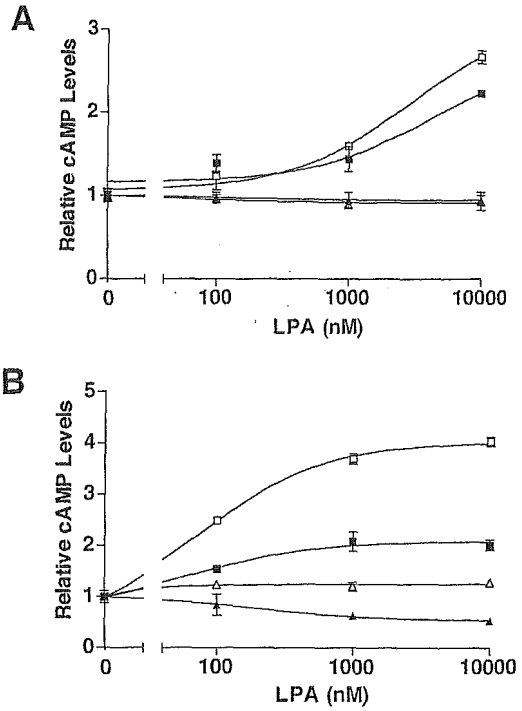

FIG. 5. **Effects of LPA on cAMP accumulation in CHO cells.** *A*, dose-response curves. A clonal population of CHO cells stably expressing $p2y_9$/GPR23 was stimulated with increasing concentrations of 18:1-LPA in the presence of 0.5 mM isobutylmethylxanthine. The cAMP contents are presented (■). The effect of pertussis toxin pretreatment on cAMP accumulation is also shown (□). The results of mock-transfected CHO cells are displayed as a negative control (▲, pertussis toxin-untreated cells; △, pertussis toxin-treated cells). cAMP levels are expressed as -fold increases above basal contents. Data are means ± S.D. (n = 4). *B*, effects of forskolin on cAMP accumulation. Cells were stimulated with 18:1-LPA in the presence of 5 μM forskolin. Assay was performed in the same manner as *A*. *Symbols* are expressed as in *A*. Data are means ± S.D. (n = 4).

onic fibroblast cells (10). They reported that Edg-7/LPA_3 was not detected by Northern blotting or reverse transcriptase-PCR in these cells. Second, RH7777 cells that do not express Edg-2/LPA_1, Edg-4/LPA_2, or Edg-7/LPA_3 have a mitogenic response to LPA and LPA analogs (12). Third, LPA-induced platelet aggregation showed different ligand specificities with Edg receptor-mediated response; the platelet response lacks the stereoselectivity (11), requires micromolar concentrations of LPA (11), and displays a distinct ligand selectivity with a preference to 1-alkyl-LPAs (13). Here we identified $p2y_9$/GPR23 as the fourth LPA receptor (LPA_4).

$p2y_9$/GPR23 was identified as a novel G protein-coupled receptor from an analysis of the expressed sequence tag (EST) data base, and the complete clone was isolated from human genomic DNA (25, 26). The $p2y_9$/GPR23 gene is located on chromosome X, region q13-q21.1, and contains an intronless open reading frame of 1113 bp encoding 370 amino acids (25, 26). However, information is limited regarding the specific ligands, tissue distribution, and biological functions of this orphan receptor.

Membrane fractions of RH7777 cells transiently transfected with $p2y_9$/GPR23 had a specific binding activity for 18:1-LPA with a K_d value of 44.8 nM (Fig. 2, *A* and *B*). Competition assays displayed the binding affinity with a rank order of 18:1- > 18:0- > 1-alkyl- > 1-alkenyl-LPA (Fig. 2*D*). This order was consistent with that of the luciferase activity: 18:1- > 18:0- > 16:0- > 14:0- > 1-alkyl- > 1-alkenyl-LPA (Fig. 3). These results indicate that 1-acyl-LPA is a better ligand for $p2y_9$/GPR23 than 1-alkyl- or 1-alkenyl-LPA, like the

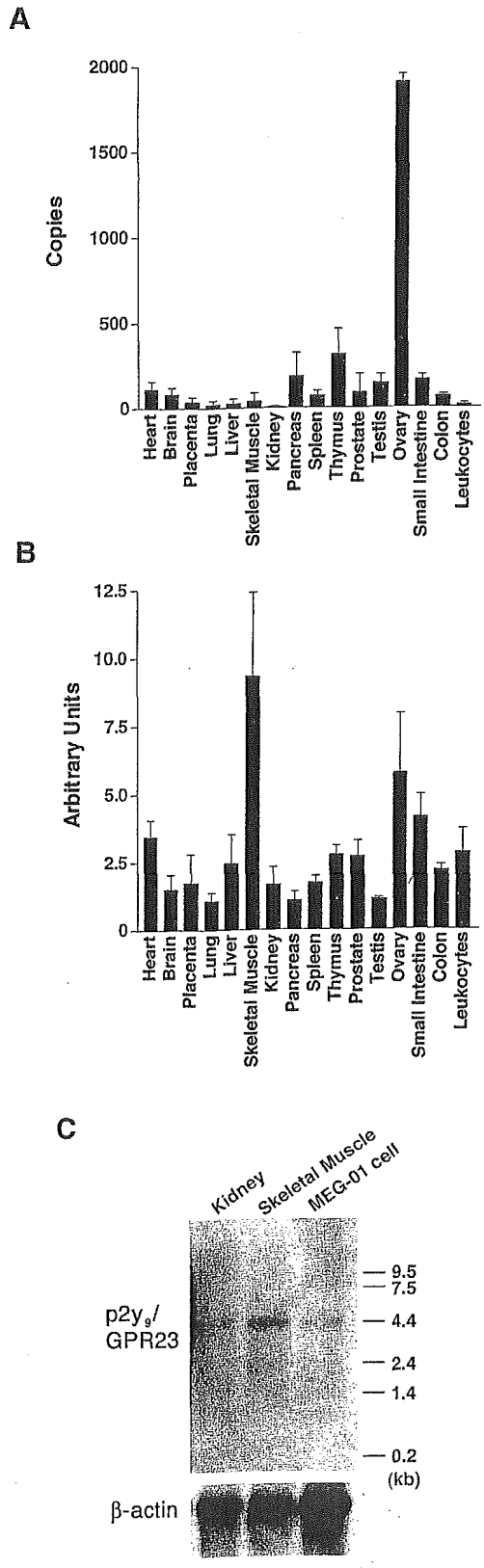

FIG. 6. **Expression of p2y$_9$/GPR23 mRNA.** *A*, quantitative real-time PCR in 16 human tissues. Expression levels of p2y$_9$/GPR23 mRNA are presented with the number of cDNA molecules initially involved in 2 μl of the template solutions. *Bars* show the mean ± S.D. of three independent experiments. *B*, expression levels of GAPDH mRNA. Quantitative real-time PCR was performed for GAPDH mRNA. Data are presented in arbitrary units. *Bars* show the means ± S.D. of three independent experiments. *C*, Northern blot analysis. Human poly(A)$^+$ RNAs (2.5 μg) were electrophoretically separated, transferred to a nylon membrane, and hybridized sequentially with [^{32}P]dCTP-labeled probes of human p2y$_9$/GPR23 and human β-actin.

previously identified LPA receptors (Edg-2/LPA$_1$, Edg-4/LPA$_2$, and Edg-7/LPA$_3$) (27, 28). Furthermore, Im *et al.* (29) showed that, among 1-acyl-LPAs, 18:1-LPA was more active than 18:0-, 16:0-, and 14:0-LPA in [γ-^{35}S]GTP binding assay with Edg-4/LPA$_2$ and Edg-7/LPA$_3$.

Mock-transfected CHO cells displayed an increase in $[Ca^{2+}]_i$ (Fig. 4, *B* and *C*), possibly due to the presence of endogenous LPA receptors. Despite this background response of CHO cells, the stable expression of p2y$_9$/GPR23 significantly enhanced the LPA-induced Ca^{2+} response by ~2-fold (Fig. 4*B*) in four independent clones. These results strongly suggest that p2y$_9$/GPR23 could elicit an intracellular Ca^{2+} mobilization, a well documented cellular effect of LPA (27).

In mock-transfected CHO cells, LPA induced a decrease in cAMP levels in the presence of forskolin, which was inhibited by pretreatment of the cells with pertussis toxin (Fig. 5*B*), suggesting the existence of endogenous LPA receptors coupling with pertussis toxin-sensitive G protein ($G_{i/o}$). By contrast, LPA induced an increase in cAMP levels in p2y$_9$/GPR23-expressing CHO cells, and pretreatment of the cells with pertussis toxin further potentiated the LPA-induced cAMP accumulation (Fig. 5, *A* and *B*). It is, therefore, possible that p2y$_9$/GPR23 is coupled with G_s, and that the effect of LPA on p2y$_9$/GPR23 is unmasked by blocking the pertussis toxin-sensitive signals from endogenous LPA receptors in CHO cells. Muscarinic M_2 and somatostatin sst_5 receptors are coupled with G_i, inhibiting adenylyl cyclase in CHO cells. However, at higher agonist concentrations, these receptors can also mediate activation of adenylyl cyclase by a mechanism involving G_s activation (30, 31). Conversely, at lower concentrations of LPA, p2y$_9$/GPR23 might inhibit the production of cAMP via G_i, like Edg-2/LPA$_1$, Edg-4/LPA$_2$, and Edg-7/LPA$_3$ (2, 3).

We also found that forskolin facilitated LPA-induced cAMP accumulation in p2y$_9$/GPR23-expressing CHO cells (Fig. 5, *A* and *B*). At least ten types of mammalian adenylyl cyclase are at present identified (32). All types of adenylyl cyclase are activated by G_s and by forskolin, and some types of adenylyl cyclase (type II, IV, V, and VI) are synergistically activated in the presence of both G_s and forskolin (32). One possible explanation of our results is that the latter types of adenylyl cyclase might be involved in the LPA-induced cAMP accumulation in p2y$_9$/GPR23-expressing CHO cells. Indeed, type VI and type VII adenylyl cyclases are expressed in CHO cells (33).

The mRNA levels of p2y$_9$/GPR23 were significantly high in ovary (Fig. 6). Various species of LPA such as linoleic, arachidonic, and docosahexaenoic acids were detected from ascites of ovarian cancer patients (24), and they had many effects on the ovarian cancer progression such as cell proliferation, prevention of apoptosis, resistance to cisplatin, and production of vascular endothelial growth factor (34). Consistently, a prominent expression of Edg-4/LPA$_2$ has been shown in primary cultures and established lines of ovarian cancer cells (35). LPA was also found at relatively high concentrations in human ovarian follicular fluid from healthy subjects (36), suggesting the relevance of LPA for normal ovarian functions as well. Tokumura (37) recently described in his review article that LPA increased the intracellular cAMP level in mouse cumulus cells. This phenomenon is consistent with our findings that the activation of p2y$_9$/GPR23 evoked cAMP accumulation in CHO cells. Thus, p2y$_9$/GPR23 might explain some of the pathological and physiological roles of LPA in ovary. It remains to be determined whether the expression of p2y$_9$/GPR23 is modulated in ovarian cancer cells. Although the EST cDNA encoding p2y$_9$/GPR23 was originally isolated from human brain (25, 26), high expression of p2y$_9$/GPR23 was not detected in brain in our study. It is possible that specific types of cells in re-

stricted areas express p2y$_9$/GPR23, which will be examined by *in situ* hybridization in the near future.

Interestingly, p2y$_9$/GPR23 shares only 20–24% amino acid identities with Edg-2/LPA$_1$, Edg-4/LPA$_2$, and Edg-7/LPA$_3$. Phylogenetic analysis also shows that p2y$_9$/GPR23 is far distant from the Edg family (Fig. 1). These facts suggest that p2y$_9$/GPR23 has evolved from ancestor sequences that are different from those of the Edg family. There are several examples of structurally unrelated receptors recognizing the same ligand. Prostaglandin D_2 binds to DP and CRTH2 (38) and histamine has four structurally distant receptors, H_1–H_4 (39). In addition, some neurotransmitters and nucleotides have both metabotropic (G protein-coupled) and ionotropic (ion channel) receptors. These examples show a limitation of the ligand search strategy utilizing a structural similarity of receptor.

As described above, there are some reports implying the existence of additional receptors for LPA. It is possible that LPA-induced responses in embryonic fibroblast cells of Edg-2/LPA$_1^{(-/-)}$ Edg-4/LPA$_2^{(-/-)}$ double knockout mice (10) might be mediated by p2y$_9$/GPR23, although we do not have any direct evidence. However, a mitogenic response to LPA in RH7777 cells (12) might be due to the activity of intracellular receptors (40), rather than G protein-coupled receptor, because mock-transfected RH7777 cells exhibited no significant binding to [^{3}H]LPA (Fig. 2*A*). As to the putative LPA receptor in platelets (11, 13), there may be a receptor other than p2y$_9$/GPR23, because the ligand preference of platelets to 1-alkyl-LPAs is not consistent with that of p2y$_9$/GPR23. Existence of further unidentified LPA receptors is, therefore, expected.

In conclusion, we report here the identification of p2y$_9$/GPR23 as a novel fourth LPA receptor (LPA$_4$). Cells expressing p2y$_9$/GPR23 displayed intracellular Ca^{2+} mobilization, cAMP accumulation, and luciferase activation. The K_d value of p2y$_9$/GPR23 (45 nM) was equivalent to those of Edg-4/LPA$_2$ (73.6 nM) and Edg-7/LPA$_3$ (206 nM) (9). Although p2y$_9$/GPR23 mRNA was significantly detected in ovary, its biological functions *in vivo* remain to be determined. Nevertheless, the present findings introduce a further complexity for LPA and its receptors. In addition, our study shows a limitation of the "de-orphaning" strategy based on the receptor structure.

Acknowledgments—We thank Dr. T. Yokomizo and H. Hagiya (The University of Tokyo) for vital discussions and critical suggestions. We are also grateful to Dr. J. Miyazaki (Osaka University, Japan) for supplying pCXN2, and H. Shindou for expert technique of binding assay.

REFERENCES

1. Tokumura, A. (1995) *Prog. Lipid Res.* **34,** 151–184
2. Contos, J. J., Ishii, I., and Chun, J. (2000) *Mol. Pharmacol.* **58,** 1188–1196
3. Fukushima, N., Ishii, I., Contos, J. J., Weiner, J. A., and Chun, J. (2001) *Annu. Rev. Pharmacol. Toxicol.* **41,** 507–534
4. Tigyi, G., and Miledi, R. (1992) *J. Biol. Chem.* **267,** 21360–21367
5. Aoki, J., Taira, A., Takanezawa, Y., Kishi, Y., Hama, K., Kishimoto, T., Mizuno, K., Saku, K., Taguchi, R., and Arai, H. (2002) *J. Biol. Chem.* **277,** 48737–48744
6. Pages, C., Simon, M. F., Valet, P., and Saulnier-Blache, J. S. (2001) *Prostaglandins Other Lipid Mediat.* **64,** 1–10
7. Hecht, J. H., Weiner, J. A., Post, S. R., and Chun, J. (1996) *J. Cell Biol.* **135,** 1071–1083
8. An, S., Bleu, T., Hallmark, O. G., and Goetzl, E. J. (1998) *J. Biol. Chem.* **273,** 7906–7910
9. Bandoh, K., Aoki, J., Hosono, H., Kobayashi, S., Kobayashi, T., Murakami-Murofushi, K., Tsujimoto, M., Arai, H., and Inoue, K. (1999) *J. Biol. Chem.* **274,** 27776–27785
10. Contos, J. J., Ishii, I., Fukushima, N., Kingsbury, M. A., Ye, X., Kawamura, S., Brown, J. H., and Chun, J. (2002) *Mol. Cell. Biol.* **22,** 6921–6929
11. Gueguen, G., Gaige, B., Grevy, J. M., Rogalle, P., Bellan, J., Wilson, M., Klaebe, A., Pont, F., Simon, M. F., and Chap, H. (1999) *Biochemistry* **38,** 8440–8450
12. Hooks, S. B., Santos, W. L., Im, D. S., Heise, C. E., Macdonald, T. L., and Lynch, K. R. (2001) *J. Biol. Chem.* **276,** 4611–4621
13. Tokumura, A., Sinomiya, J., Kishimoto, S., Tanaka, T., Kogure, K., Sugiura, T., Satouchi, K., Waku, K., and Fukuzawa, K. (2002) *Biochem. J.* **365,** 617–628
14. Nakamura, M., Honda, Z., Izumi, T., Sakanaka, C., Mutoh, H., Minami, M., Bito, H., Seyama, Y., Matsumoto, T., Noma, M., and Shimizu, T. (1991) *J. Biol. Chem.* **266,** 20400–20405
15. Niwa, H., Yamamura, K., and Miyazaki, J. (1991) *Gene (Amst.)* **108,** 193–199
16. Ogasawara, H., Ishii, S., Yokomizo, T., Kakinuma, T., Komine, M., Tamaki, K., Shimizu, T., and Izumi, T. (2002) *J. Biol. Chem.* **277,** 18763–18768
17. Boeynaems, J. M., Communi, D., Savi, P., and Herbert, J. M. (2000) *Trends Pharmacol. Sci.* **21,** 1–3
18. Hla, T., Lee, M. J., Ancellin, N., Paik, J. H., and Kluk, M. J. (2001) *Science* **294,** 1875–1878
19. Fukushima, N., Kimura, Y., and Chun, J. (1998) *Proc. Natl. Acad. Sci. U. S. A.* **95,** 6151–6156
20. Ogura, M., Morishima, Y., Ohno, R., Kato, Y., Hirabayashi, N., Nagura, H., and Saito, H. (1985) *Blood* **66,** 1384–1392
21. Baker, D. L., Desiderio, D. M., Miller, D. D., Tolley, B., and Tigyi, G. J. (2001) *Anal. Biochem.* **292,** 287–295
22. Sugiura, T., Nakane, S., Kishimoto, S., Waku, K., Yoshioka, Y., Tokumura, A., and Hanahan, D. J. (1999) *Biochim. Biophys. Acta* **1440,** 194–204
23. Liliom, K., Guan, Z., Tseng, J. L., Desiderio, D. M., Tigyi, G., and Watsky, M. A. (1998) *Am. J. Physiol.* **274,** C1065–C1074
24. Xu, Y., Gaudette, D. C., Boynton, J. D., Frankel, A., Fang, X. J., Sharma, A., Hurteau, J., Casey, G., Goodbody, A., and Mellors, A. (1995) *Clin. Cancer Res.* **1,** 1223–1232
25. O'Dowd, B. F., Nguyen, T., Jung, B. P., Marchese, A., Cheng, R., Heng, H. H., Kolakowski, L. F., Jr., Lynch, K. R., and George, S. R. (1997) *Gene (Amst.)* **187,** 75–81
26. Janssens, R., Boeynaems, J. M., Godart, M., and Communi, D. (1997) *Biochem. Biophys. Res. Commun.* **236,** 106–112
27. An, S., Bleu, T., Zheng, Y., and Goetzl, E. J. (1998) *Mol. Pharmacol.* **54,** 881–888
28. Bandoh, K., Aoki, J., Taira, A., Tsujimoto, M., Arai, H., and Inoue, K. (2000) *FEBS Lett.* **478,** 159–165
29. Im, D. S., Heise, C. E., Harding, M. A., George, S. R., O'Dowd, B. F., Theodorescu, D., and Lynch, K. R. (2000) *Mol. Pharmacol.* **57,** 753–759
30. Carruthers, A. M., Warner, A. J., Michel, A. D., Feniuk, W., and Humphrey, P. P. (1999) *Br. J. Pharmacol.* **126,** 1221–1229
31. Michal, P., Lysikova, M., and Tucek, S. (2001) *Br. J. Pharmacol.* **132,** 1217–1228
32. Sunahara, R. K., Dessauer, C. W., and Gilman, A. G. (1996) *Annu. Rev. Pharmacol. Toxicol.* **36,** 461–480
33. Varga, E. V., Stropova, D., Rubenzik, M., Wang, M., Landsman, R. S., Roeske, W. R., and Yamamura, H. I. (1998) *Eur. J. Pharmacol.* **348,** R1–R2
34. Fang, X., Gaudette, D., Furui, T., Mao, M., Estrella, V., Eder, A., Pustilnik, T., Sasagawa, T., Lapushin, R., Yu, S., Jaffe, R. B., Wiener, J. R., Erickson, J. R., and Mills, G. B. (2000) *Ann. N. Y. Acad. Sci.* **905,** 188–208
35. Goetzl, E. J., Dolezalova, H., Kong, Y., and Zeng, L. (1999) *Cancer Res.* **59,** 4732–4737
36. Jaspard, B., Collet, X., Barbaras, R., Manent, J., Vieu, C., Parinaud, J., Chap, H., and Perret, B. (1996) *Biochemistry* **35,** 1352–1357
37. Tokumura, A. (2002) *Biochim. Biophys. Acta* **1582,** 18–25
38. Hirai, H., Tanaka, K., Yoshie, O., Ogawa, K., Kenmotsu, K., Takamori, Y., Ichimasa, M., Sugamura, K., Nakamura, M., Takano, S., and Nagata, K. (2001) *J. Exp. Med.* **193,** 255–261
39. Schneider, E., Rolli-Derkinderen, M., Arock, M., and Dy, M. (2002) *Trends Immunol.* **23,** 255–263
40. McIntyre, T. M., Pontsler, A. V., Silva, A. R., St. Hilaire, A., Xu, Y., Hinshaw, J. C., Zimmerman, G. A., Hama, K., Aoki, J., Arai, H., and Prestwich, G. D. (2003) *Proc. Natl. Acad. Sci. U. S. A.* **100,** 131–136

Improved Host Defense against Pneumococcal Pneumonia in Platelet-Activating Factor Receptor–Deficient Mice

Anita W. Rijneveld,[1,2] Sebastiaan Weijer,[1,2] Sandrine Florquin,[3] Peter Speelman,[2,4] Takao Shimizu,[5] Satosh Ishii,[5] and Tom van der Poll[1,4]

[1]Laboratory of Experimental Internal Medicine and Departments of [2]Internal Medicine, [3]Pathology, and [4]Infectious Diseases, Tropical Medicine, and AIDS, Academic Medical Center, University of Amsterdam, Amsterdam, The Netherlands; [5]Department of Biochemistry and Molecular Biology, Faculty of Medicine, University of Tokyo, and CREST of Japan Science and Technology Corporation, Tokyo, Japan

Platelet-activating factor (PAF) is a phospholipid with proinflammatory properties that binds to a specific receptor (PAF receptor [PAFR]) that is expressed on many different cell types. PAFR is able to bind phosphorylcholine, which is present in both PAF and the pneumococcal cell wall. Activation of respiratory epithelial cells in vitro results in up-regulation of PAFR, which, in turn, facilitates invasion of *Streptococcus pneumoniae*. To determine the role of PAFR in host defense against pneumococcal pneumonia, PAFR-deficient ($PAFR^{-/-}$) and wild-type *(wt)* mice were inoculated intranasally with *S. pneumoniae*. $PAFR^{-/-}$ mice were relatively resistant to pneumococcal pneumonia, as indicated by delayed and reduced mortality, diminished outgrowth of pneumococci in lungs, and reduced dissemination of the infection (all $P < .05$, vs. *wt* mice). $PAFR^{-/-}$ mice also had less pulmonary inflammation. These data provide evidence that PAFR is used by *S. pneumoniae* to induce lethal pneumonia.

Platelet-activating factor (PAF) is a glycerophospholipid produced mainly by platelets, endothelial cells, macrophages, and neutrophils that plays an important role in the orchestration of different inflammatory reactions [1–3]. The biological activity of PAF is mediated through a specific G-protein–linked receptor (PAF receptor [PAFR]) that is expressed on different cell types, including neutrophils, monocytes, macrophages, and epithelial cells. Via PAFR, PAF exerts several immunomodulatory actions involved in host defense against bacterial infections, including stimulation of migration and degranulation of granulocytes, monocytes, and macrophages and the release of cytokines and toxic oxygen metabolites [1–3].

PAFR has been thought to play a crucial role in the pathogenesis of pneumococcal disease [4]. The biological activity of PAF is mainly determined by phosphorylcholine (PC), which binds specifically to PAFR [1–3]; PC is also a prominent part of the cell wall of *Streptococcus pneumoniae* [5]. Activation of endothelial or epithelial cells results in up-regulation of PAFR at their surface, which, in turn, facilitates invasion by *S. pneumoniae* via an interaction between PAFR and the PC component of the pneumococcal cell wall [6–8]. The relevance in vivo of the interaction between pneumococcal PC and PAFR is supported by several findings. First, administration of either a PAFR antagonist or an anti-PC antibody reduced leukocytosis and protein concentrations in the cerebrospinal fluid of rabbits injected intracisternally with *S. pneumoniae* [9]. Second, administration of a PAFR antagonist also reduced the recruitment of leukocytes and the increase in protein concentrations in bronchoalveolar lavage (BAL) fluid (BALF) of rabbits challenged intratracheally (int) with killed *S. pneumoniae* [9]. Third, the combination

Received 19 February 2003; accepted 29 June 2003; electronically published 30 January 2004.

Financial support: Dutch Association for Scientific Research (grants to A.W.R. and S.W.); Ministry of Health, Labour, and Welfare, Japan (grants-in-aid for comprehensive research on aging and health and for research on allergic disease and immunology to S.I.).

Reprints or correspondence: Dr. Anita W. Rijneveld, Academic Medical Center, University of Amsterdam, F4-105, Meibergdreef 9, 1105 AZ Amsterdam, The Netherlands (a.w.rijneveld@amc.uva.nl).

The Journal of Infectious Diseases 2004;189:711–6

0022-1899/2004/18904-0020$15.00